



AS2070: Aerospace Structural Mechanics

Module 3: Introduction to Fatigue and Failure (V9)

Instructor: Nidish Narayanaa Balaji

Department of Aerospace Engineering, IIT Madras

April 24, 2026

Table of Contents

Also see <https://www.fracturemechanics.org/>

1 Introduction

- Structure of Materials
- Understanding the Stress-Strain Curve
- Failure Mechanisms
 - Fracture
 - Fatigue
- Energy Release Rate
- Linear Elastic Fracture Mechanics
- Modes of Fracture

2 Introduction to Failure

- Maximum Shear Stress Theory
- Distortion Energy Theory
- Maximum Normal Stress Theory

3 Introduction to Fatigue

- The Parameters of Fatigue Testing
- Miner's Rule
- The deHavilland Comet

4 Linear Elastic Fracture Mechanics

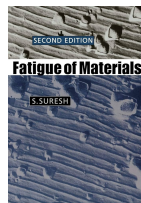
- A Primer on 2D Elasticity
- Classical Solutions
 - Plate with a Hole Under Uniaxial Tension
 - Plate with a Hole Under Biaxial Tension
 - Notch Crack
- Griffith's Analysis and Energy Release Rate
 - The Notch Crack Revisited
- Crack Propagation in Practice
- The Plastic Zone - A Primer on Elastic Plastic Fracture Mechanics
- Things We Have Not Considered

5 Tutorial Problems

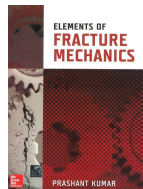
- Stress for Fatigue Life Estimation
Balaji, N. N. (AE, IITM)



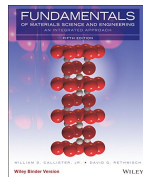
Chapters 1,4
in Gdoutos (2005)



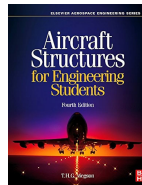
Chapters 1,7,9
in Suresh (1998)



Chapters 1-3
in Kumar (2009)



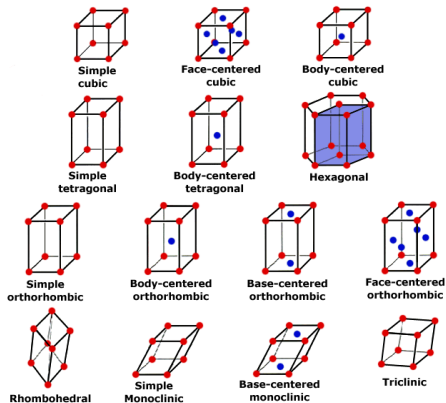
Chapter 3,5,6
in Jr and
Rethwisch (2012)



Chapter 15
in Megson (2013)

1.1. Structure of Materials

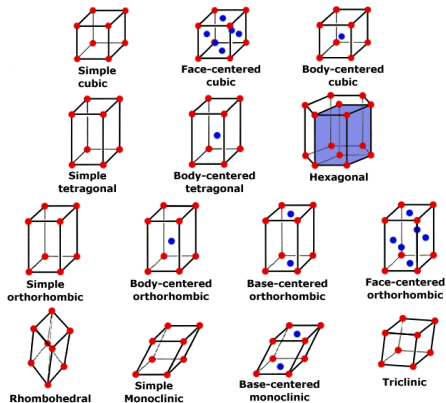
Introduction



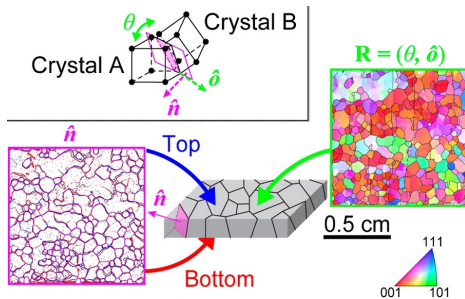
Types of crystal structures in metals Sparky (2013)

1.1. Structure of Materials

Introduction



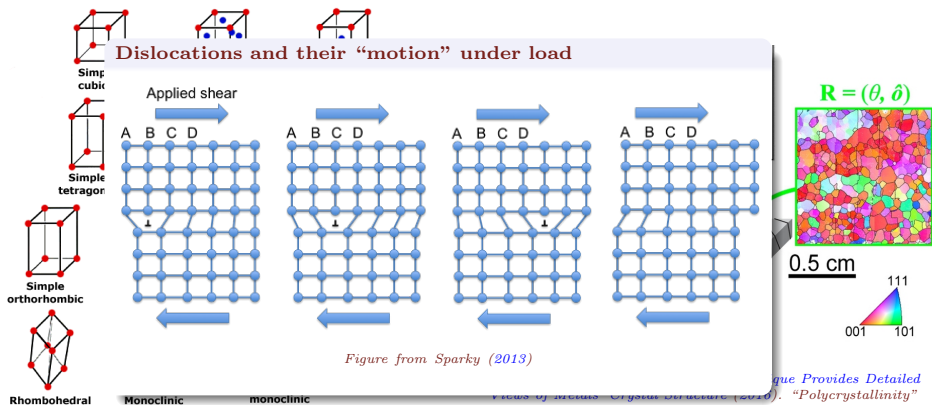
Types of crystal structures in metals Sparky (2013)



Crystal and Grain Structures New Technique Provides Detailed Views of Metals' Crystal Structure (2016). "Polycrystallinity"

1.1. Structure of Materials

Introduction



Types of crystal structures in metals Sparky (2013)

1.2. Understanding the Stress-Strain Curve

Introduction

The Uniaxial Tensile Test

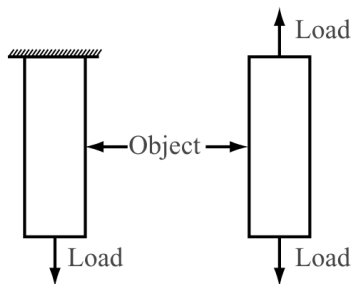


Figure from Rajendran 2011

1.2. Understanding the Stress-Strain Curve

Introduction

Terminology

- ➊ Proportionality Limit;
- ➋ Elastic Limit;
- ➌ Yield Point;
- ➍ Ultimate Strength;
- ➎ Fracture Point;
- ➏ Elongation at Failure;

Ductile Fracture

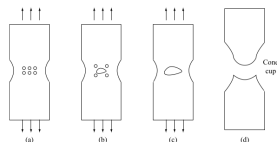


Figure from Rajendran 2011

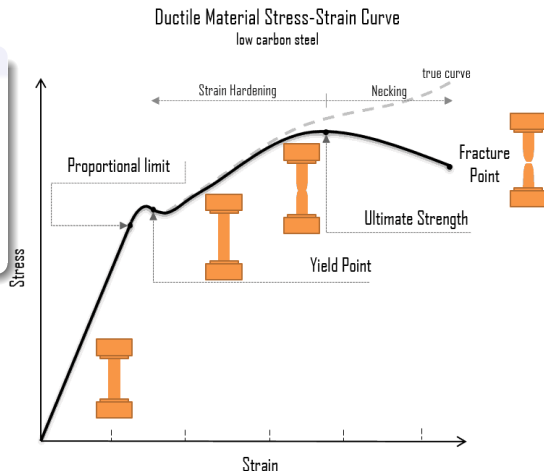


Figure from Connor 2020

1.3. Failure Mechanisms: Fracture

1. Introduction

“Griffith Theory” of brittle fracture

- Theoretical fracture stress $\sim \frac{E}{5} - \frac{E}{30}$
(steel $\sim \frac{E}{1000}$)
- Fracture occurs when
 $E_{strain} = E_{surface}$
- Crack propagates when
 $\frac{dE_{strain}}{dL} = \frac{dE_{surface}}{dL}$

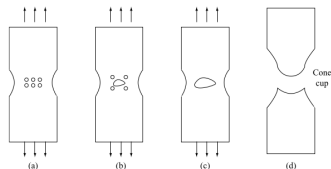
1.3. Failure Mechanisms: Fracture

1. Introduction

“Griffith Theory” of brittle fracture

- Theoretical fracture stress $\sim \frac{E}{5} - \frac{E}{30}$
(steel $\sim \frac{E}{1000}$)
- Fracture occurs when
 $E_{strain} = E_{surface}$
- Crack propagates when
 $\frac{dE_{strain}}{dL} = \frac{dE_{surface}}{dL}$

Ductile Fracture



Ductile Fracture Rajendran 2011

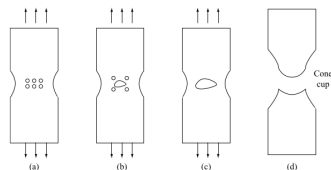
1.3. Failure Mechanisms: Fracture

1. Introduction

“Griffith Theory” of brittle fracture

- Theoretical fracture stress $\sim \frac{E}{5} - \frac{E}{30}$
(steel $\sim \frac{E}{1000}$)
- Fracture occurs when
 $E_{strain} = E_{surface}$
- Crack propagates when
 $\frac{dE_{strain}}{dL} = \frac{dE_{surface}}{dL}$

Ductile Fracture



Ductile Fracture Rajendran 2011

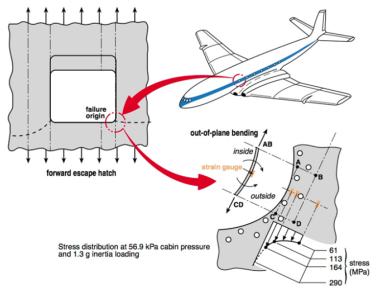
Sr. No	Brittle Fracture	Ductile Fracture
1.	It occurs with no or little plastic deformation.	It occurs with large plastic deformation.
2.	The rate of propagation of the crack is fast.	The rate of propagation of the crack is slow.
3.	It occurs suddenly without any warning.	It occurs slowly.
4.	The fractured surface is flat.	The fractured surface has rough contour and the shape is similar to cup and cone arrangement.
5.	The fractured surface appears shiny.	The fractured surface is dull when viewed with naked eye and the surface has dimpled appearance when viewed with scanning electron microscope.
6.	It occurs where micro crack is larger.	It occurs in localised region where the deformation is larger.

Ductile vs Brittle Fracture Rajendran 2011

1.3. Failure Mechanisms: Fatigue

1. Introduction

..over 90% of mechanical failures are caused because of metal fatigue *What Is Metal Fatigue?*
2021...



*The De Havilland Comet The deHavilland Comet Disaster
2019 [lecture]*

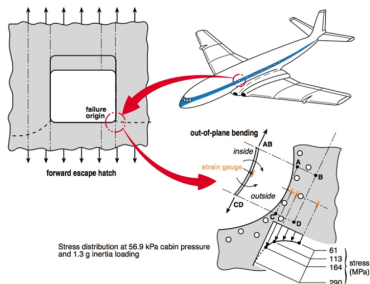
1.3. Failure Mechanisms: Fatigue

1. Introduction

..over 90% of mechanical failures are caused because of metal fatigue *What Is Metal Fatigue?* 2021...



A more recent example (2021 United Airlines Boeing 777) [DCA21FA085.Aspx](#) 2024. [\[video\]](#)



The De Havilland Comet *The deHavilland Comet Disaster* 2019 [\[lecture\]](#)

1.3. Failure Mechanisms: Fatigue

1. Introduction

..over 90% of mechanical failures are caused because of metal fatigue *What Is Metal Fatigue?*
2021...



A more recent example
777) *DCA21FAug08.Asp* 2024. [\[video\]](#)

Fatigue Crack Propagation: Beech Marks

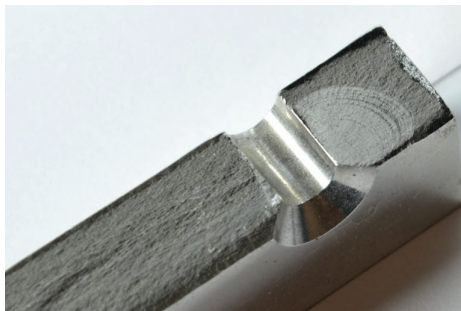
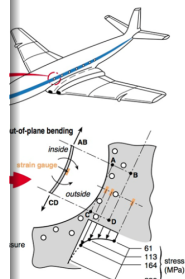


Figure from *Fatigue Physics 2024*

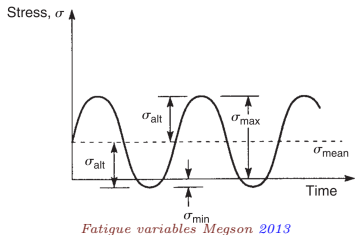


deHavilland Comet Disaster
[\[structure\]](#)

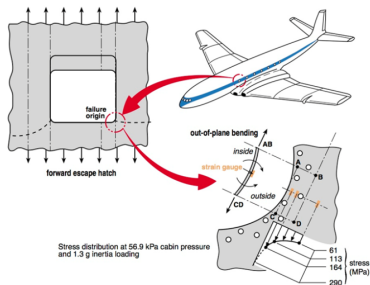
1.3. Failure Mechanisms: Fatigue

1. Introduction

..over 90% of mechanical failures are caused because of metal fatigue *What Is Metal Fatigue?*
2021...



Fatigue variables Megson 2013

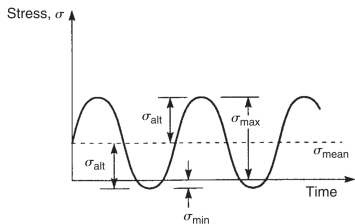


The De Havilland Comet The deHavilland Comet Disaster 2019 [lecture]

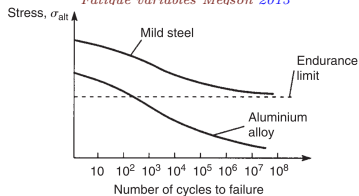
1.3. Failure Mechanisms: Fatigue

1. Introduction

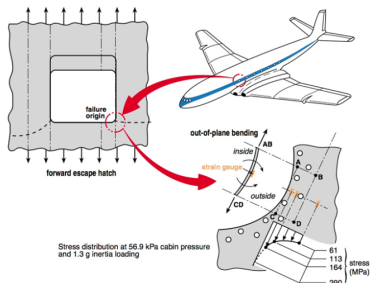
..over 90% of mechanical failures are caused because of metal fatigue *What Is Metal Fatigue?*
2021...



Fatigue variables Meason 2013



The S-n Diagram Meason 2013



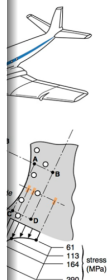
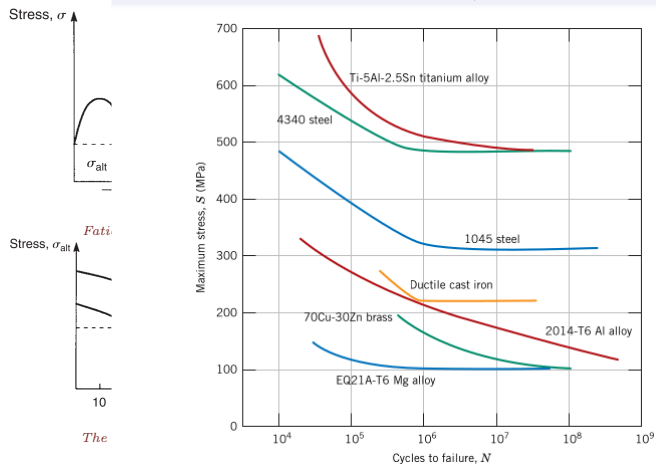
The De Havilland Comet The deHavilland Comet Disaster 2019 [lecture]

1.3. Failure Mechanisms: Fatigue

1. Introduction

..over 90% of mechanical failures are caused because of metal fatigue *What Is Metal Fatigue?* 2021...

S-N Curves for Common Metals (Jr and Rethwisch 2012)



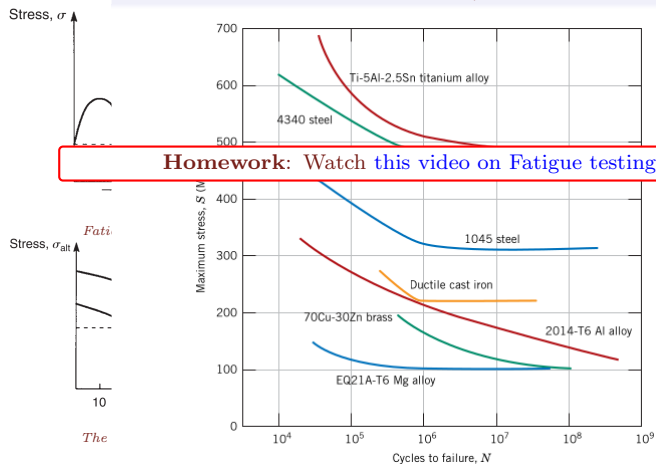
Comet Disaster

1.3. Failure Mechanisms: Fatigue

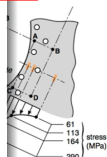
1. Introduction

..over 90% of mechanical failures are caused because of metal fatigue *What Is Metal Fatigue?* 2021...

S-N Curves for Common Metals (Jr and Rethwisch 2012)



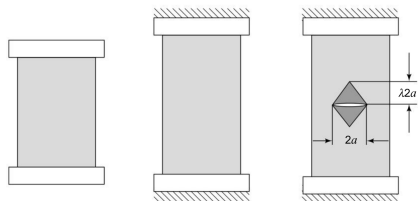
Homework: Watch [this video on Fatigue testing.](#)



Comet Disaster

1.4. Energy Release Rate: Griffith's Analysis

Introduction



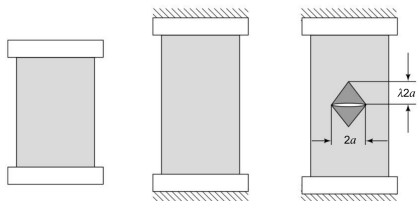
Simplistic picture of the introduction of a crack in a stretched specimen (Figure from sec 2.5 in Kumar 2009)

- Because of the crack, we assume $\sigma \approx 0$ in the triangles.
- Corresponding energy loss:

$$E_R = V_{\Delta} \times \left(\frac{\sigma^2}{2E} \right) = \frac{2a^2 \lambda t \sigma^2}{E}.$$

1.4. Energy Release Rate: Griffith's Analysis

Introduction



Simplistic picture of the introduction of a crack in a stretched specimen (Figure from sec 2.5 in Kumar 2009)

- Because of the crack, we assume $\sigma \approx 0$ in the triangles.
- Corresponding energy loss:

$$E_R = V_{\Delta} \times \left(\frac{\sigma^2}{2E} \right) = \frac{2a^2 \lambda t \sigma^2}{E}.$$

- For thin plates, $\lambda = \frac{\pi}{2}$. So,

$$E_R = \frac{\pi a^2 t \sigma^2}{E}.$$

- The “creation” of a surface takes energy. We write this as,

$$E_S = 2(2at)\gamma = 4at\gamma.$$

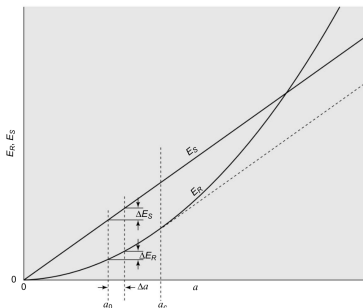
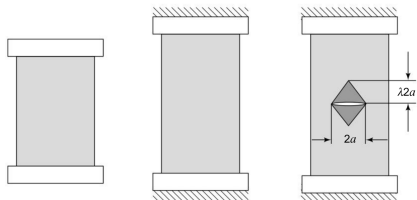


(Figure from Kumar 2009)

1.4. Energy Release Rate: Griffith's Analysis

Introduction



Simplistic picture of specimen (Figure from Kumar 2009)

- Because of the triangular crack tip

- Corresponding energy loss:

$$E_R = V_{\Delta} \times \left(\frac{\sigma^2}{2E} \right) = \frac{2a^2 \lambda t \sigma^2}{E}.$$

Food For Thought

- What would a “safe size” of crack be, for a given loading condition? *Hint: Think incrementally*

- For thin plates, $\lambda = \frac{\pi}{2}$. So,

$$E_R = \frac{\pi a^2 t \sigma^2}{E}.$$

- The “creation” of a surface takes energy. We write this as,

$$E_S = 2(2at)\gamma = 4at\gamma.$$

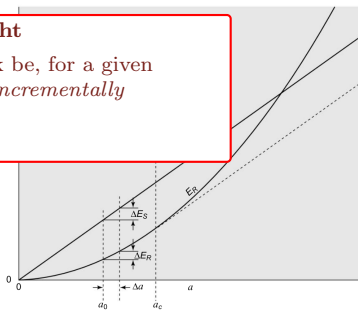
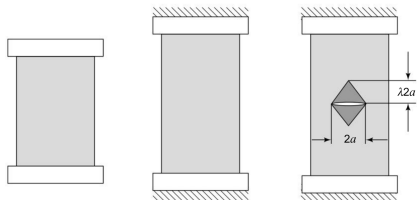


(Figure from Kumar 2009)

1.4. Energy Release Rate: Griffith's Analysis

Introduction



Simplistic picture of specimen (Figure from Griffith 1920)

- Because of the triangular crack tip region
- Corresponding energy loss:

$$E_R = V_{\Delta} \times \left(\frac{\sigma^2}{2E} \right) = \frac{2a^2 \lambda t \sigma^2}{E}$$

Food For Thought

- What would a “safe size” of crack be, for a given loading condition? *Hint: Think incrementally*
- What type of an experiment would be necessary to confirm this mathematical framework?

- For thin plates, $\lambda = \frac{\pi}{2}$. So,

$$E_R = \frac{\pi a^2 t \sigma^2}{E}$$

- The “creation” of a surface takes energy. We write this as,

$$E_S = 2(2at)\gamma = 4at\gamma.$$

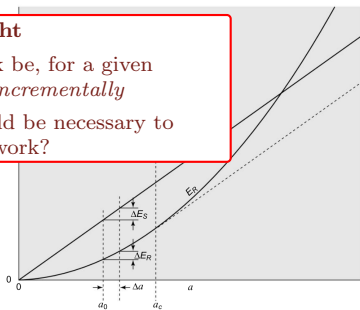


(Figure from Kumar 2009)

1.5. Linear Elastic Fracture Mechanics

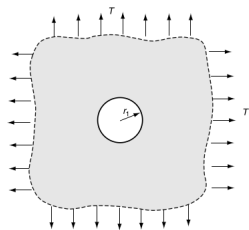
Introduction

(Ref: Sec. 8.4.2 in Sadd 2009)

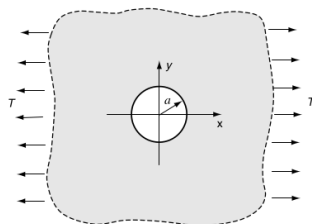
Consider the following two cases.

Question: Where will the point of peak stress occur? And which will have higher maximum stress?

Case 1



Case 2



1.5. Linear Elastic Fracture Mechanics

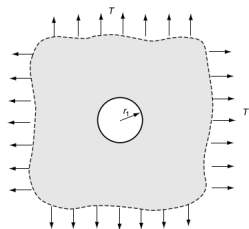
Introduction

(Ref: Sec. 8.4.2 in Sadd 2009)

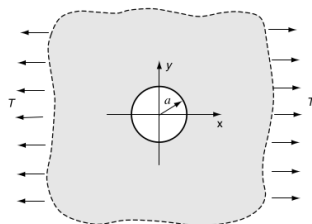
Consider the following two cases.

Question: Where will the point of peak stress occur? And which will have higher maximum stress?

Case 1



Case 2



Analytical Solution

$$\sigma_r = T\left(1 - \frac{r_1^2}{r^2}\right), \quad \sigma_\theta = T\left(1 + \frac{r_1^2}{r^2}\right)$$

$$\Rightarrow \boxed{\sigma_{\max} = 2T}$$

1.5. Linear Elastic Fracture Mechanics

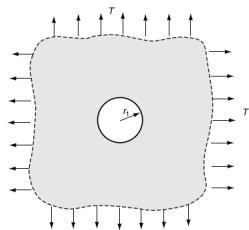
Introduction

(Ref: Sec. 8.4.2 in Sadd 2009)

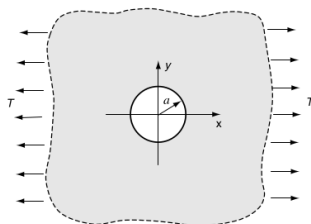
Consider the following two cases.

Question: Where will the point of peak stress occur? And which will have higher maximum stress?

Case 1



Case 2



Analytical Solution

$$\sigma_r = T\left(1 - \frac{r_1^2}{r^2}\right), \quad \sigma_\theta = T\left(1 + \frac{r_1^2}{r^2}\right)$$

$$\Rightarrow \sigma_{\max} = 2T$$

Analytical Solution

$$\sigma_r = T\left(1 - \frac{r_1^2}{r^2}\right) + (\cdot) \cos(2\theta), \quad \sigma_\theta = \dots$$

$$\Rightarrow \sigma_{\max} = 3T$$

1.5. Linear Elastic Fracture Mechanics

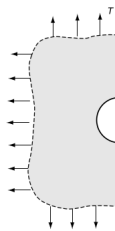
Introduction

(Ref: Sec. 8.4.2 in Sadd 2009)

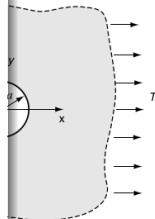
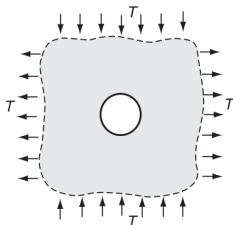
Consider the following two cases.

Question: Where will the point of peak stress occur? And which will have higher maximum stress?

Case 1



Case 3



Analytical Solution

$$\sigma_r = T\left(1 - \frac{r_1^2}{r^2}\right), \quad \sigma_\theta = T\left(1 + \frac{r_1^2}{r^2}\right)$$

$$\Rightarrow \sigma_{\max} = 2T$$

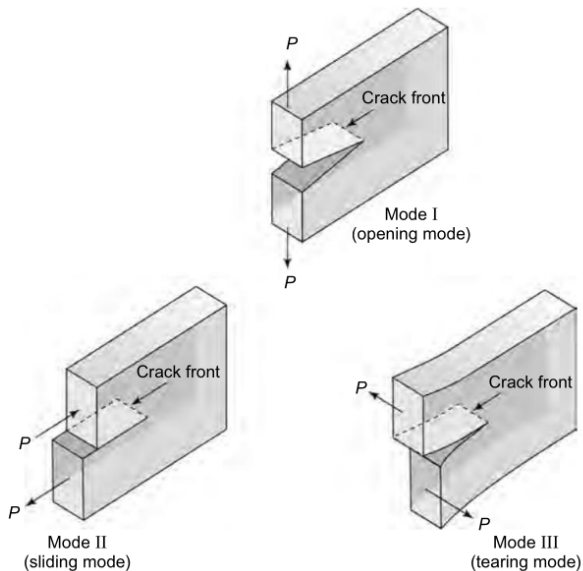
$$\sigma_{\max} = 4T$$

$$\sigma_r = T\left(1 - \frac{r_1^2}{r^2}\right) + (\cdot) \cos(2\theta), \quad \sigma_\theta = \dots$$

$$\Rightarrow \sigma_{\max} = 3T$$

1.6. Modes of Fracture

Introduction



2. Introduction to Failure

Necessary Reading: Secs. 5-3 to 5-9
in Budynas, Nisbett, and Shigley 2015

- Elasticity only deals with the **reversible deformation** behavior. But real materials undergo yielding, necking, and eventually failure under large loads.
- Since there is permanent loss during the yield process (irreversibility), we will have to abandon **non-dissipativity** and modify the stress-strain relationship.

An Approach for a Failure Theory...

- **Conduct** controlled experiments in the lab
- **Observe** characteristics of failure
- **Propose generalizations** and test with further experimentation



Failed mild steel specimens (under uni-axial tension)

2. Introduction to Failure

- A first observation is that materials can be classified as brittle or ductile based on whether they undergo a plastic yield before failure.
- Generally, a material is said to be
 - **Ductile** if strain at failure is greater than 5%,
 - **Brittle** if strain at failure is lesser than 5%.
- For **Ductile Materials** the commonly applicable theories are
 - **Maximum Shear Stress Theory (MSS)**: Failure occurs when the maximum shear stress reaches a threshold. (aka **Tresca theory**)
 - **Distortion Energy Theory (DE)**: Failure occurs when the distortional strain energy reaches a threshold.
 - **Ductile Coulomb-Mohr (DCM) Theory**: The shear stress threshold for failure grows linearly with straight stress. *Proposed to account for tensile and compressive strengths being different*
- For **Brittle Materials** the applicable theories are
 - **Maximum Normal Stress Theory (MNS)**: Failure occurs when the normal stress reaches a threshold.
 - **Brittle Columb-Mohr (BCM) Theory**: Same idea as in DCM, to account for different tensile and compressive strengths.
- We will only bother ourselves with MSS, DE, and MNS here.

2.1. Maximum Shear Stress Theory

Introduction to Failure

- For ductile materials, failure in a uniaxial tensile test almost always involves a plane at 45° from the direction of loading.
- From the Mohr circle relationships for the uniaxial case at yielding point ($\sigma_1 = S_y, \sigma_2 = 0$) we have,

$$\sigma_n = \frac{S_y}{2} + \frac{S_y}{2} \cos 2\theta, \quad \tau_s = -\frac{S_y}{2} \sin 2\theta.$$

- We empirically observe that the $\theta = 45^\circ$ also corresponds to the plane where the shear traction component is maximum!

We **hypothesize** that

...yielding begins whenever the maximum shear stress in any element equals or exceeds the maximum shear stress in a tension-test specimen of the same material when that specimen begins to yield.



Failed mild steel specimens (under uni-axial tension) ◀ ◻ ▶

2.1. Maximum Shear Stress Theory

Introduction to Failure

- For ductile materials, failure in a uniaxial tensile test almost always involves a plane at 45° from the direction of loading.
- From the Mohr circle relationships for the uniaxial case at yielding point ($\sigma_1 = S_y, \sigma_2 = 0$) we have,

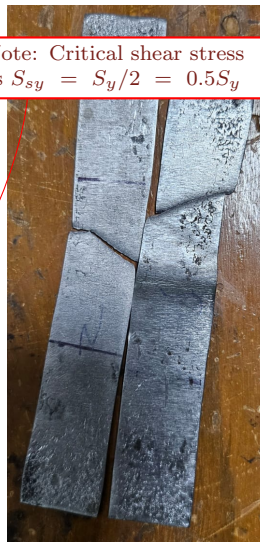
$$\sigma_n = \frac{S_y}{2} + \frac{S_y}{2} \cos 2\theta, \quad \tau_s = -\frac{S_y}{2} \sin 2\theta.$$

- We empirically observe that the $\theta = 45^\circ$ also corresponds to the plane where the shear traction component is maximum!

We **hypothesize** that

...yielding begins whenever the maximum shear stress in any element equals or exceeds the maximum shear stress in a tension-test specimen of the same material when that specimen begins to yield.

Note: Critical shear stress is $S_{sy} = S_y/2 = 0.5S_y$



Failed mild steel specimens (under uni-axial tension) ◀ ◻ ▶

2.1. Maximum Shear Stress Theory

Introduction to Failure

- For ductile materials, failure in a uniaxial tensile test almost always involves a plane at 45° from the direction of loading.
- From the Mohr circle relationships for the uniaxial case at yielding point ($\sigma_1 = S_y, \sigma_2 = 0$) we have,

$$\sigma_n = \frac{S_y}{2} + \frac{S_y}{2} \cos 2\theta, \quad \tau_s = -\frac{S_y}{2} \sin 2\theta.$$

- **We empirically observe that the $\theta = 45^\circ$ also corresponds to the plane where the shear traction component is maximum!**

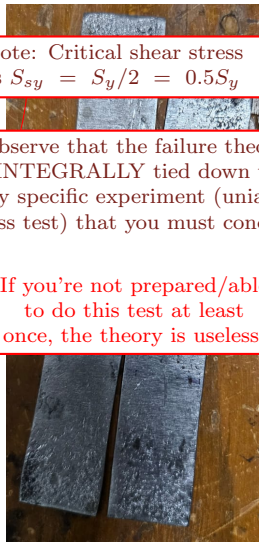
We **hypothesize** that

...yielding begins whenever the maximum shear stress in any element equals or exceeds the maximum shear stress in a tension-test specimen of the same material when that specimen begins to yield.

Note: Critical shear stress is $S_{sy} = S_y/2 = 0.5S_y$

Observe that the failure theory is **INTEGRALLY** tied down to a very specific experiment (uniaxial stress test) that you must conduct.

If you're not prepared/able to do this test at least once, the theory is useless.



Failed mild steel specimens (under uni-axial tension) ◀ ◻ ▶

2.1. Maximum Shear Stress Theory: Application to Bi-Axial Loading

Introduction to Failure

- For a general case, all of σ_1 , σ_2 and σ_3 are non-zero.
- The maximum shear stress that can be achieved (among all possible planes) is $\tau_{\max} = \frac{\sigma_1 - \sigma_2}{2}$. MSS predicts that failure will happen when $\tau_{\max} \geq 0.5S_y$, i.e.,

$$\boxed{|\sigma_1 - \sigma_2| \geq S_y}, \boxed{|\sigma_1 - \sigma_3| \geq S_y}, \boxed{|\sigma_2 - \sigma_3| \geq S_y}.$$

Note that for the 2D case we will take $\sigma_3 = 0$.

- We've got the “non-yield region” in the σ_1, σ_2 space to be:

$$\{(\sigma_1, \sigma_2) \mid |\sigma_1 - \sigma_2| < S_y, |\sigma_1| < S_y, |\sigma_2| < S_y\}$$

- **So given a general state of stress $\underline{\underline{\sigma}}$, we must first estimate the principal stresses and check if they fall within the above to check if it would fail according to the MSS/Tresca theory.**

2.1. Maximum Shear Stress Theory: Application to Bi-Axial Loading

Introduction to Failure

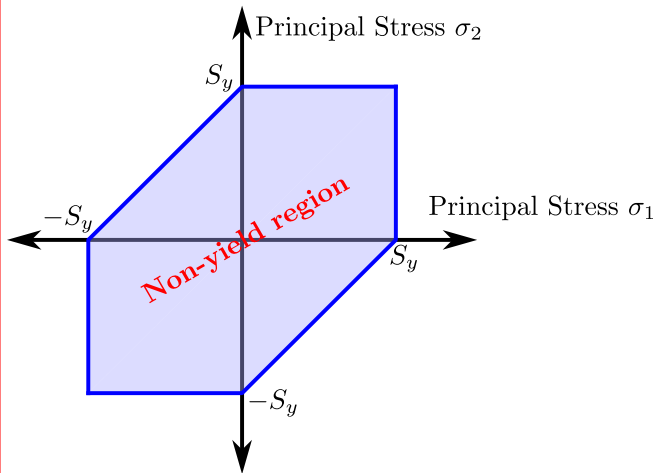
Graphical Depiction of the Non-Yield Region from MSS

- For a ge
- The max
- $\tau_{\max} =$

) is
i.e.,

Note tha

- We've go
- So give
- stresses
- accordi

Principal
d fail

2.2. Distortion Energy Theory

Introduction to Failure

- We **hypothesize here** that shape change energy is what leads to failure, **NOT isotropic volume change**.
- So we “remove” the volume change energy from the overall energy and require that the remaining energy (which we will call as “distortional” since this only represents shape change) does not exceed the energy contained in a uniaxial test context.

Formally we hypothesize that

yielding occurs when the distortion strain energy per unit volume reaches or exceeds the distortion strain energy per unit volume for yield in simple tension or compression of the same material.

2.2. Distortion Energy Theory

Introduction to Failure

- The total energy for a general state of stress in an isotropic material is given by:

$$\mathcal{U} = \frac{1}{2E_Y} [\sigma_1 \quad \sigma_2 \quad \sigma_3] \begin{bmatrix} 1 & -\nu & -\nu \\ -\nu & 1 & -\nu \\ -\nu & -\nu & 1 \end{bmatrix} \begin{bmatrix} \sigma_1 \\ \sigma_2 \\ \sigma_3 \end{bmatrix} = \frac{1}{2E_Y} (\sigma_1^2 + \sigma_2^2 + \sigma_3^2 - 2\nu(\sigma_1\sigma_2 + \sigma_1\sigma_3 + \sigma_2\sigma_3))$$

- The work done by the “hydrostatic pressure” is written by replacing each σ_i by $\sigma_{av} = \frac{\sigma_1 + \sigma_2 + \sigma_3}{3}$:

$$\mathcal{U}_v = \frac{3(1-2\nu)}{2E_Y} \sigma_{av}^2 = \frac{1-2\nu}{6E_Y} (\sigma_1^2 + \sigma_2^2 + \sigma_3^2 + 2(\sigma_1\sigma_2 + \sigma_1\sigma_3 + \sigma_2\sigma_3)).$$

\mathcal{U}_v is interpreted as energy that only goes into volume change.

- The shape change/distortional energy is the “remaining energy” after taking \mathcal{U}_v out of \mathcal{U} :

$$\mathcal{U}_d = \mathcal{U} - \mathcal{U}_v = \frac{1+\nu}{E_Y} \left(\frac{(\sigma_1 - \sigma_2)^2 + (\sigma_1 - \sigma_3)^2 + (\sigma_2 - \sigma_3)^2}{2} \right).$$

- A uniaxial tensile test specimen fails when the state of stress is $(\sigma_1, \sigma_2, \sigma_3) = (S_y, 0, 0)$. The corresponding distortional energy is written as

$$\mathcal{U}_{d,y} = \frac{1+\nu}{E_Y} S_y^2 \implies \boxed{\mathcal{U}_d < \mathcal{U}_{d,y}} \text{ to avoid yielding.}$$

2.2. Distortion Energy Theory

Introduction to Failure

Take a Second to Interpret!

- Mathematical Summary:

$$\sqrt{\frac{(\sigma_1 - \sigma_2)^2 + (\sigma_1 - \sigma_3)^2 + (\sigma_2 - \sigma_3)^2}{2}} < S_y$$

- An alternative interpretation of this theory comes from the fact that the shear stress magnitude on an octahedral plane (plane with normal $\hat{n} = \frac{1}{\sqrt{3}} [1 \ 1 \ 1]^T$) is the same as the LHS above.
- Sometimes referred to as the **Maximum Octahedral Stress Theory**, this states that failure happens due to shear on an octahedral plane. It is mathematically identical to DE.
- It is interesting to note that the epistemology of failure is actually not our concern here - we are merely interested in putting our uniaxial tensile testing data to good use in a way that captures the uniaxial tensile test itself as just a sub-case !

$$U_{d,y} = \frac{1+\nu}{E_Y} S_y^2 \implies U_d < U_{d,y} \text{ to avoid yielding.}$$

2.2. Distortion Energy Theory

Introduction to Failure

- For the plane stress situation ($\sigma_1 \neq 0, \sigma_2 \neq 0, \sigma_3 = 0$), the non-yield region is given by

$$\{(\sigma_1, \sigma_2) \mid \frac{(\sigma_1 - \sigma_2)^2 + \sigma_1^2 + \sigma_2^2}{2} \leq S_y^2\},$$

which defines a rotated ellipse in 2D.

- For a state of “pure shear” of magnitude τ , the principal stresses are $\sigma_1 = \tau, \sigma_2 = -\tau$. Here, the criterion becomes,

$$3\tau^2 \leq S_y^2 \implies S_{sy} = \frac{S_y}{\sqrt{3}} = 0.577S_y.$$

2.2. Distortion Energy Theory

Introduction to Failure

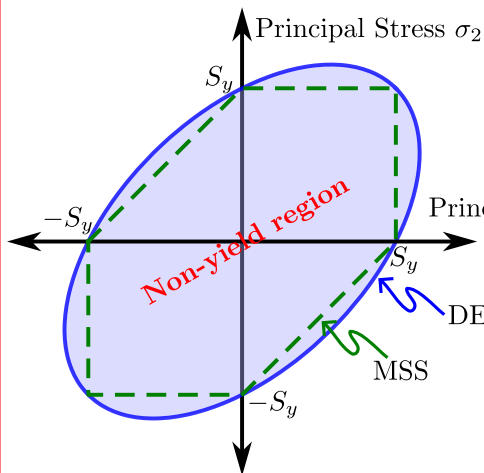
Graphical Depiction of the Non-Yield Region from DE & MSS

- For the p

is given by

which de

- For a sta
- Here, the

 $\tau_1, \sigma_2 = -\tau$.

2.2. Distortion Energy Theory

Introduction to Failure

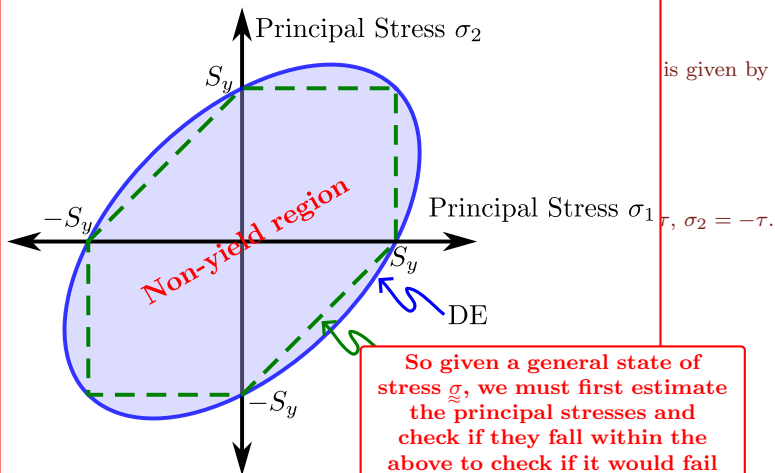
Graphical Depiction of the Non-Yield Region from DE & MSS

- For the p

is given by

which de

- For a sta
- Here, the



So given a general state of stress $\underline{\sigma}$, we must first estimate the principal stresses and check if they fall within the above to check if it would fail according to the DE theory.

2.2. Distortion Energy Theory

Introduction to Failure

- For the plane stress situation ($\sigma_1 \neq 0, \sigma_2 \neq 0, \sigma_3 = 0$), the non-yield region is given by

$$\{(\sigma_1, \sigma_2) \mid \frac{(\sigma_1 - \sigma_2)^2 + \sigma_1^2 + \sigma_2^2}{2} \leq S_y^2\},$$

which defines a rotated ellipse in 2D.

- For a state of “pure shear” of magnitude τ , the principal stresses are $\sigma_1 = \tau, \sigma_2 = -\tau$. Here, the criterion becomes,

$$3\tau^2 \leq S_y^2 \implies S_{sy} = \frac{S_y}{\sqrt{3}} = 0.577S_y.$$

What about **Plane Strain**? Will there be any difference?

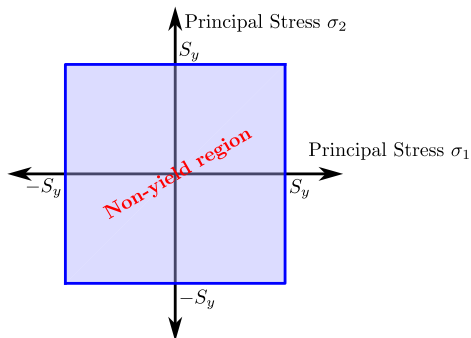
2.3. Maximum Normal Stress Theory

Introduction to Failure

We hypothesize that

yielding occurs when the **maximum normal stress** in any element equals or exceeds the maximum normal stress in a tension-test specimen of the same material when that specimen begins to yield.

- The hypothesis follows in the same vein as the previous two theories - following experimental experience with brittle material fracture which happens, on tensile test specimens, on a plane perpendicular to the direction of loading.



3. Introduction to Fatigue

- It is sometimes the case that components in machinery fail even though no part of them has ever experienced stresses that violated any of the above failure theory envelopes!
- This is known as **Fatigue**, and pertains to failure under repetitive stress cycles.
- Remind yourself that we are **NOT** very much concerned with the epistemology (they “why”) of this phenomenon: We have observed this, and we want to use this knowledge in design. This will be our approach.
- Plotting the **stress-amplitude-to-failure** against the **number-of-cycles-to-failure** leads to the famous “Strength-Cycles/S-n Curve” of fatigue.

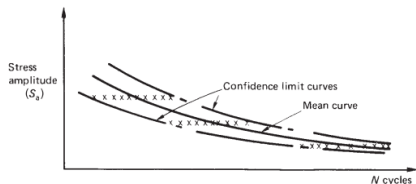
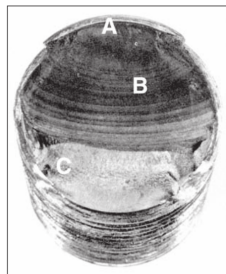


(Figure 15.1 from Megson 2013)

Figure 6-1

Fatigue failure of a bolt due to repeated unidirectional bending. The failure started at the thread root at A, propagated across most of the cross section shown by the beach marks at B, before final fast fracture at C. (From ASM Handbook, Vol. 12: Fractography, 2nd printing, 1992, ASM International, Materials Park, OH 44073-0002, fig 50, p. 120. Reprinted by permission of ASM International[®], www.asminternational.org.)



Beach marks (Figure 6-1 from Budynas, Nisbett, and Shigley 2015)

3. Introduction to Fatigue

- It is sometimes the case that components in machinery fail even though no part of them has ever experienced stresses that violated any of the above failure theory envelopes!

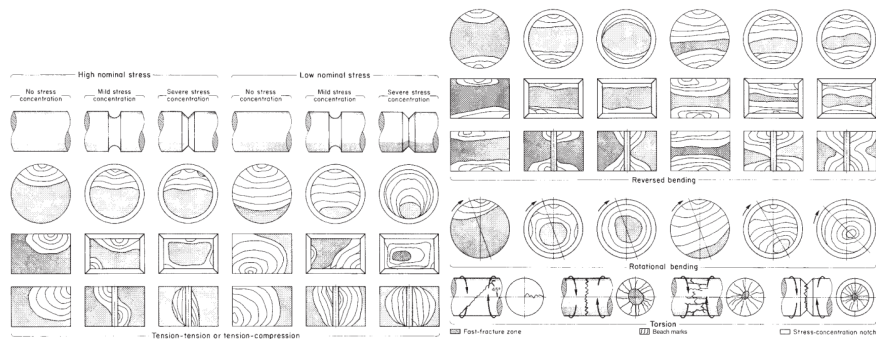
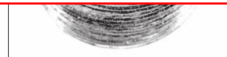


(Figure 6-1 from Budynas, Nisbett, and Shigley 2015)

N cycles

(Figure 15.1 from Megson 2013)

1993-0002, fig. 50, p. 120.
Reprinted by permission
of ASM International®,
www.asminternational.org.)



Beach marks (Figure 6-1 from Budynas, Nisbett, and Shigley 2015)

3. Introduction to Fatigue

- It is sometimes the case that a component has never experienced a stress level that is above the failure theory envelopes!

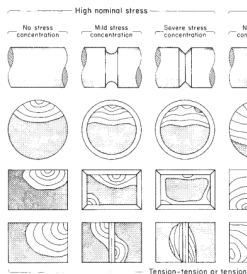


(Figure 15.1 from Megawick)

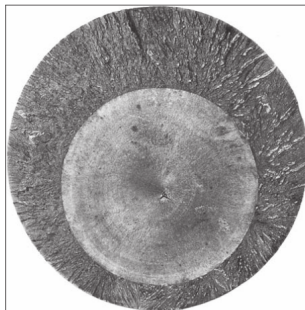
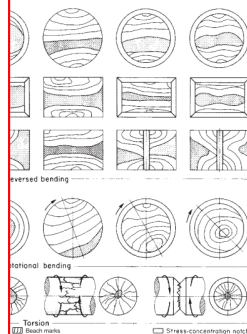


Figure 6-6

Fatigue fracture surface of a 200-mm (8-in) diameter piston rod of an alloy steel steam hammer used for forging. This is an example of a fatigue fracture caused by pure tension where surface stress concentrations are absent and a crack may initiate anywhere in the cross section. In this instance, the initial crack formed at a forging flake slightly below center, grew outward symmetrically, and ultimately produced a brittle fracture without warning. (From ASM Handbook, Vol. 12: Fractography, 2nd printing, 1992, ASM International, Materials Park, OH 44073-0002, fig 570, p. 342. Reprinted by permission of ASM International[®], www.asminternational.org.)

(Figure 6-6 from Budynas, Nisbett, and Shigley 2015)

- Even though no part of them has ever experienced a stress level that is above the failure theory envelopes!



Beach marks (Figure 6-1 from Budynas, Nisbett, and Shigley 2015)

3.1. The Parameters of Fatigue Testing

Introduction to Fatigue

- We characterize fluctuating stress in terms of the max and min stress values σ_{\max} , σ_{\min} or the derived quantities:

$$\text{Midrange Stress } \sigma_m = \frac{\sigma_{\min} + \sigma_{\max}}{2}$$

$$\text{Alternating Stress } \sigma_a = \left| \frac{\sigma_{\max} - \sigma_{\min}}{2} \right|$$

$$\text{Range of Stress } \sigma_r = \sigma_{\max} - \sigma_{\min}$$

$$\text{Steady Stress } \sigma_u$$

- In general, we only plot the alternating stress σ_a versus the cycles to failure in the S-n curve.

Figure 6-10

An S-N diagram plotted from the results of completely reversed axial fatigue tests. Material: UNS G41300 steel, normalized; $S_u = 116$ kpsi; maximum $S_w = 125$ kpsi. (Data from NACA Tech. Note 3866, December 1966.)

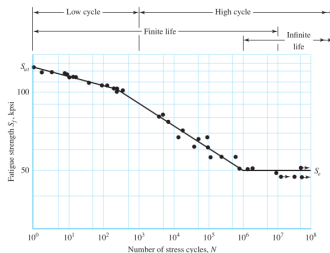


Figure 6-10 from Budynas, Nisbett, and Shigley 2015

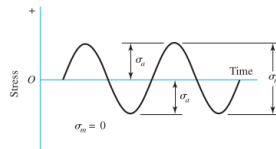
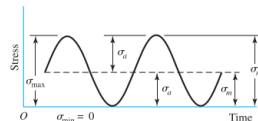
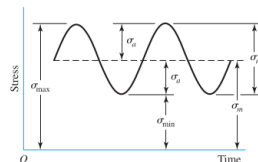
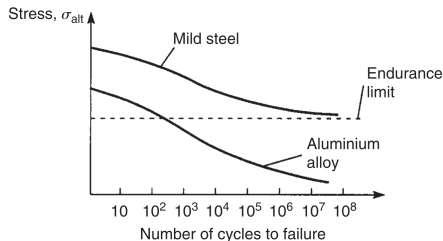


Figure 6-23 from Budynas, Nisbett, and Shigley 2015

3.1. The Parameters of Fatigue Testing: Two Useful Parameterizations for HCF

Introduction to Fatigue

- High Cycle Fatigue (HCF) is characterized by regions where number of cycles to failure exceeds 10^3 .



(Figure from Megson 2013)

- One of the simplest formulae (not necessarily very accurate) to capture the trend is the Basquin formula (1910):

$$\sigma_a = \sigma'_f (2N)^b, \quad b < 0.$$

- σ'_f is the fatigue strength coefficient, sometimes set to equal the ultimate tensile strength σ_{ult} .
- b is the power law coefficient - $b_1 < b_2$ implies material 1 shows more rapid strength drop-off than material 2.

3.1. The Parameters of Fatigue Testing: Two Useful Parameterizations for HCF

Introduction to Fatigue

- High Cycle Fatigue (HCF) is characterized by regions where number of cycles to failure exceeds 10^3 .

Stress, σ_{alt} ↑
Mild steel

Typical Basquin coefficients σ'_f and b for selected materials

Material	σ'_f (MPa)	b
Mild steel (low carbon)	400 – 800	-0.06 to -0.10
Cast iron (grey)	200 – 500	-0.05 to -0.08
Aluminium alloys (wrought)	300 – 700	-0.06 to -0.11
Aluminium alloys (cast)	150 – 350	-0.07 to -0.13
Titanium alloys	800 – 2000	-0.08 to -0.13
Nickel superalloys	1000 – 2500	-0.06 to -0.10
CFRP (composites)	500 – 1500	-0.04 to -0.10

- One of the parameters in the Basquin equation is the

- σ'_f is the fatigue strength coefficient, sometimes set to equal the ultimate tensile strength σ_{ult} .
- b is the power law coefficient - $b_1 < b_2$ implies material 1 shows more rapid strength drop-off than material 2.

3.1. The Parameters of Fatigue Testing

Introduction to Fatigue

- The Basquin relationship predicts that the stress to failure at infinite cycles is zero. Clearly this is incapable of predicting the endurance limit.
- So a modified (Stromeyer) formula is used for alloys that show a finite endurance limit:

$$\sigma_a(N) = AN^b + \sigma_e.$$

Typical Stromeyer coefficients for $\sigma_a = aN^b + \sigma_e$

Material	a (MPa)	b	σ_e (MPa)
Mild steel	900 – 1200	–0.10 to –0.12	200 – 280
Cast iron (grey)	400 – 700	–0.08 to –0.10	100 – 150
Al alloys (wrought)	400 – 600	–0.10 to –0.13	—
Al alloys (cast)	200 – 400	–0.10 to –0.15	—
Titanium alloys	1200 – 2500	–0.08 to –0.12	400 – 650
Nickel superalloys	1500 – 3000	–0.07 to –0.10	500 – 800
CFRP	800 – 1800	–0.06 to –0.10	—

— No endurance limit; $\sigma_e = 0$ (pure power law applies).

- **Necessary Reading:** Ch. 6 in Budynas, Nisbett, and Shigley [2015](#)
- **Recommended Reading:** Murakami et al. [2021](#)

3.1. The Parameters of Fatigue Testing

Introduction to Fatigue

- In order to make the results from the S-n curve more practical, I will ask the following question:

For a required life of N cycles, what combinations of midrange (σ_m) and alternating (σ_a) stresses may be deemed safe?

- The Goodman relationship (1890) offers a simple formula for the maximum safe alternating stress σ_a for given mid-range stress σ_m

$$\frac{\sigma_a}{\sigma_{a0}} = 1 - \left(\frac{\sigma_m}{S_{ult}} \right)^m$$

with coefficient m to be determined experimentally.

Here, σ_{a0} is the zero-mean alternating stress level where the system fails after N cycles. S_{ult} is the ultimate strength of the material.

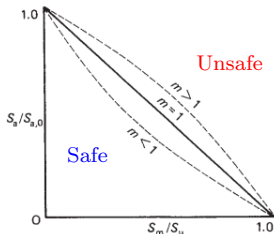


(Figure 15.2 from Megson 2013)

3.1. The Parameters of Fatigue Testing

Introduction to Fatigue

- In order to make the results from the S-n curve more practical, I will ask the following question:

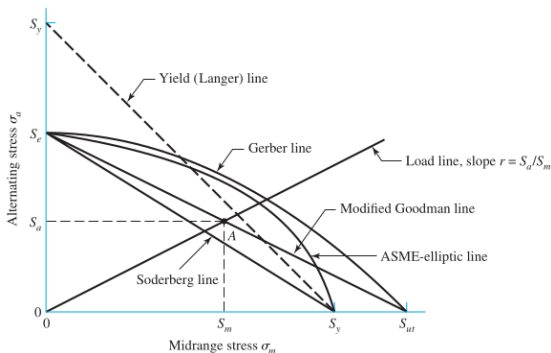
For a required number of cycles N and alternating stresses (σ_a)

- The Goodman criterion is a very crude heuristic for determining the maximum safe alternating stress σ_a for a given midrange stress σ_m .

with coefficient $r = \sigma_a / \sigma_m$.

Here, σ_{a0} is the maximum safe alternating stress after N cycles.

But please note that Fatigue looks like a **very random phenomenon** in practice. So the Goodman criterion is a very crude heuristic.



So many alternative criteria are in use Figure 6-27 from Budynas, Nisbett, and Shigley 2015

(Figure 15.2 from Megson 2013)

3.2. Miner's Rule

Introduction to Fatigue

- Suppose at an operation level of σ_m, σ_a , the fatigue life is N and the structure undergoes n cycles, Miner's rule posits that $\frac{n}{N}$ is the fraction of life that has been consumed.
- Suppose a structure undergoes multiple stress levels in its loading history, the total fraction of fatigue life that has been consumed is written as

$$\frac{n_1}{N_1} + \frac{n_2}{N_2} + \frac{n_3}{N_3} + \dots$$

- The structure is expected to fail when this sum becomes a constant c which is usually $0.7 < c < 2.2$.
- Also referred to as the **Palmgren-Miner cycle-ratio summation** rule, it is expressed as

$$\sum_i \frac{n_i}{N_i} = D.$$

- D is treated as a “damage index”. When this reaches the value of c (mostly taken as unity), we expect failure.

3.3. The deHavilland Comet

Introduction to Fatigue

No aircraft has contributed more to safety in the jet age than the Comet. The lessons it taught the world of aeronautics live in every jet airliner flying today. – D.D. Dempster, 1959, in The Tale of the Comet

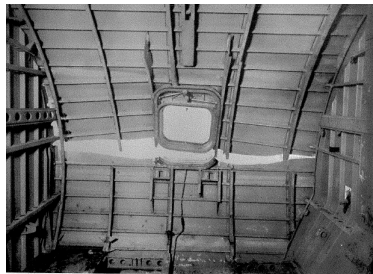


FIG. 7. VIEW FROM INSIDE OF FAILURE AT THE FORWARD ESCAPE HATCH ON THE PORT SIDE—COMET G-ALYU

(Figures from "De Havilland Comet" 2025)

3.3. The deHavilland Comet

Introduction to Fatigue

No aircraft has contributed more to safety in the jet age than the Comet. The lessons it taught the world of aeronautics live in every jet airliner flying today. – D.D. Dempster, 1959, in The Tale of the Comet.

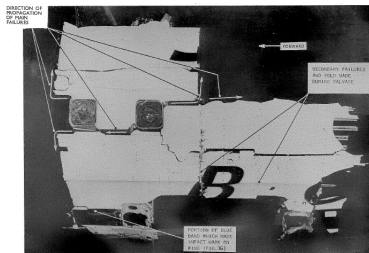


FIG. 12. PHOTOGRAPH OF WRECKAGE AROUND ADF AERIAL WINDOWS—G-ALPR.

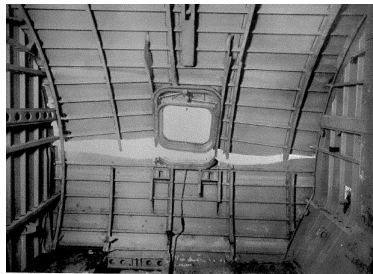


FIG. 7. VIEW FROM INSIDE OF FAILURE AT THE FORWARD ESCAPE HATCH ON THE PORT SIDE—COMET G-ALYU

(Figures from “De Havilland Comet” 2025)

3.3. The de Havilland Comet

Introduction to

No aircraft
taught the
1950s

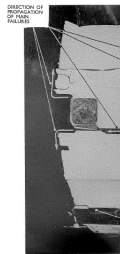
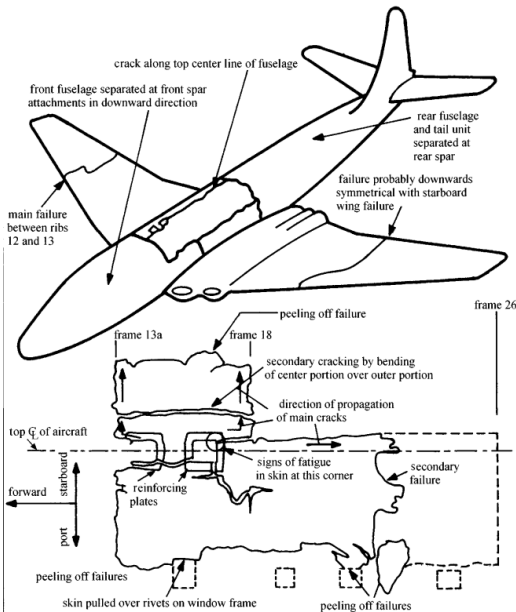


FIG. 12. PHOTO



Lessons it
tempster,



TOUCH ON THE

t" 2025)

4. Linear Elastic Fracture Mechanics

- Let us now turn our attention to **Linear Elastic Fracture Mechanics** (LEFM).
- Before actually delving into LEFM, let us just use what we already know (stress-driven failure theories - MSS, MDE, MNS) and consider the exact stress distribution for some two-dimensional cases.
- The main machinery for this comes from the so-called Airy's stress function ϕ that is governed by the *biharmonic equation* $\nabla^4\phi = 0$.
- The Airy's stress function is a powerful tool that lets us obtain the stress distribution in fully closed form.
- In particular, we will pursue this in the cylindrical coordinate system where the exact solutions can be tabulated and we can start applying superposition.

4.1. A Primer on 2D Elasticity

Linear Elastic Fracture Mechanics

- In 2D, the governing equations of elasticity (let us assume no body loads for simplicity) are written as,

$$\sigma_{x,x} + \tau_{xy,y} = 0, \quad \tau_{xy,x} + \sigma_{y,y} = 0.$$

- If we seek to obtain **solutions expressed directly in the stresses**, 2 equations won't cut it (we have 3 unique stresses $\sigma_x, \sigma_y, \tau_{xy}$). So we invoke strain compatibility, which is written as

$$\varepsilon_{x,yy} + \varepsilon_{y,xx} = \gamma_{xy,xy}$$

- This can be expressed in terms of the stresses if we invoke the **stress-strain constitutive relationships**.

4.1. A Primer on 2D Elasticity

Linear Elastic Fracture Mechanics

- In 2D, the governing equations of elasticity (let us assume no body loads for simplicity) are written as,

$$\sigma_{x,x} + \tau_{xy,y} = 0, \quad \tau_{xy,x} + \sigma_{y,y} = 0.$$

- If we seek to obtain **solutions expressed directly in the stresses**, 2 equations won't cut it (we have 3 unique stresses $\sigma_x, \sigma_y, \tau_{xy}$). So we invoke **compatibility conditions** written as

$$\varepsilon_{x,yy} + \varepsilon_{y,xx} = \gamma_{xy,xy}$$

Recall: These are conditions that the strains must satisfy in order for them to have been generated by a continuously differentiable displacement field.

- This can be expressed in terms of the stresses if we invoke the **stress-strain constitutive relationships**.

4.1. A Primer on 2D Elasticity

Linear Elastic Fracture Mechanics

Plane Stress

$$\begin{bmatrix} \varepsilon_x \\ \varepsilon_y \\ \gamma_{xy} \end{bmatrix} = \frac{1}{E} \begin{bmatrix} 1 & -\nu & 0 \\ -\nu & 1 & 0 \\ 0 & 0 & 2(1+\nu) \end{bmatrix} \begin{bmatrix} \sigma_x \\ \sigma_y \\ \tau_{xy} \end{bmatrix}$$

Compatibility

$$\sigma_{x,yy} + \sigma_{y,xx} - \nu(\sigma_{x,xx} + \sigma_{y,yy}) = 2(1+\nu)\tau_{xy,xy}.$$

Plane Strain

$$\begin{bmatrix} \varepsilon_x \\ \varepsilon_y \\ \gamma_{xy} \end{bmatrix} = \frac{1+\nu}{E} \begin{bmatrix} 1-\nu & -\nu & 0 \\ -\nu & 1-\nu & 0 \\ 0 & 0 & 2 \end{bmatrix} \begin{bmatrix} \sigma_x \\ \sigma_y \\ \tau_{xy} \end{bmatrix}$$

Compatibility

$$(1-\nu)(\sigma_{x,yy} + \sigma_{y,xx}) - \nu(\sigma_{x,xx} + \sigma_{y,yy}) = 2\tau_{xy,xy}.$$

- Making the substitution $\sigma_x = \phi_{,yy}$, $\sigma_y = \phi_{,xx}$, $\tau_{xy} = -\phi_{,xy}$, it is trivial to see that the equilibrium equations are satisfied automatically.
- In both the above cases, the compatibility equation comes out to be:

$$\phi_{,xxxx} + \phi_{,yyyy} + 2\phi_{,xxyy} = (\partial_{xx} + \partial_{yy})^2 \phi = \nabla^4 \phi = 0.$$

- Since the Laplacian when set to zero ($\nabla^2 \phi = 0$) is referred to as the **harmonic equation** (recall complex analyticity), $\nabla^4 \phi = 0$ is referred to as the **bi-harmonic equation**. ϕ is the **Airy Stress Function**.

4.2. Classical Solutions

Linear Elastic Fracture Mechanics

- Let us look at the biharmonic equation $\nabla^4 \phi = 0$ with cylindrical coordinates ($x = r \cos \theta$, $y = r \sin \theta$).

$$\underline{\nabla} \phi = \begin{bmatrix} \underline{e}_r & \underline{e}_\theta \end{bmatrix} \begin{bmatrix} \phi_{,r} \\ \phi_{,\theta} \\ r \end{bmatrix}, \quad \underline{\nabla} \underline{u} = \begin{bmatrix} \underline{e}_r & \underline{e}_\theta \end{bmatrix} \begin{bmatrix} u_{r,r} & \frac{u_{r,\theta} - u_\theta}{r} \\ u_{\theta,r} & \frac{u_{\theta,\theta} + u_r}{r} \end{bmatrix} \begin{bmatrix} \underline{e}_r \\ \underline{e}_\theta \end{bmatrix}$$

$$\underline{\nabla}^2 \phi = \begin{bmatrix} \underline{e}_r & \underline{e}_\theta \end{bmatrix} \begin{bmatrix} \phi_{,rr} & \partial_r \left(\frac{\phi_{,\theta}}{r} \right) \\ \partial_r \left(\frac{\phi_{,\theta}}{r} \right) & \frac{\phi_{,r}}{r} + \frac{\phi_{,\theta\theta}}{r^2} \end{bmatrix} \begin{bmatrix} \underline{e}_r \\ \underline{e}_\theta \end{bmatrix}.$$

- The stresses are expressed in terms of the Laplacian of ϕ to satisfy equilibrium by definition as before:

$$\sigma_{rr} = \frac{\phi_{,r}}{r} + \frac{\phi_{,\theta\theta}}{r^2}, \quad \sigma_{\theta\theta} = \phi_{,rr}, \quad \tau_{r\theta} = -\partial_r \left(\frac{\phi_{,\theta}}{r} \right).$$

- The biharmonic equation gets written as

$$\left(\frac{1}{r} \frac{\partial}{\partial r} \left(\frac{1}{r} \frac{\partial}{\partial r} \right) + \frac{1}{r^2} \frac{\partial^2}{\partial \theta^2} \right)^2 \phi = 0.$$

Unlike the Cartesian case, the general homogeneous solution for $\phi(r, \theta)$ can be expressed in closed form! This can be used to “construct” any arbitrary solution as superpositions thereof.

4.2. Classical Solutions

Linear Elastic Fracture Mechanics

- Let us look at the biharmonic equation $\nabla^4 \phi = 0$ with cylindrical coordinates ($x = r \cos \theta$, $y = r \sin \theta$).

**General form of the Airy's Stress Function
(Michell Solution, see Barber 2022, Ch. 8-9)**

$$\phi = a_0 + a_1 \log r + a_2 r^2 + a_3 r^2 \log r$$

$$(a_4 + a_5 \log r + a_6 r^2 + a_7 r^2 \log r) \theta$$

$$(a_{11} r + a_{12} r \log r + \frac{a_{13}}{r} + a_{14} r^3 + a_{15} r \theta + a_{16} r \theta \log r) \cos \theta$$

$$(b_{11} r + b_{12} r \log r + \frac{b_{13}}{r} + b_{14} r^3 + b_{15} r \theta + b_{16} r \theta \log r) \sin \theta$$

$$\sum_{n=2}^{\infty} (a_{n1} r^n + a_{n2} r^{2+n} + a_{n3} r^{-n} + a_{n4} r^{2-n}) \cos n\theta$$

$$\sum_{n=2}^{\infty} (b_{n1} r^n + b_{n2} r^{2+n} + b_{n3} r^{-n} + b_{n4} r^{2-n}) \sin n\theta.$$

$$\left(r \frac{\partial}{\partial r} \left(r \frac{\partial}{\partial r} \right) + r^2 \frac{\partial^2}{\partial \theta^2} \right) \phi = 0.$$

Unlike the Cartesian case, the general homogeneous solution for $\phi(r, \theta)$ can be expressed in closed form! This can be used to “construct” any arbitrary solution as superpositions thereof.

4.2. The Michell Solution: Tabled Expressions

Classical Solutions

Stress Components

ϕ	σ_{rr}	$\sigma_{r\theta}$	$\sigma_{\theta\theta}$
r^2	2	0	2
$r^2 \ln(r)$	$2 \ln(r) + 1$	0	$2 \ln(r) + 3$
$\ln(r)$	$1/r^2$	0	$-1/r^2$
θ	0	$1/r^2$	0
$r^3 \cos \theta$	$2r \cos \theta$	$2r \sin \theta$	$6r \cos \theta$
$r\theta \sin \theta$	$2 \cos \theta / r$	0	0
$r \ln(r) \cos \theta$	$\cos \theta / r$	$\sin \theta / r$	$\cos \theta / r$
$\cos \theta / r$	$-2 \cos \theta / r^3$	$-2 \sin \theta / r^3$	$2 \cos \theta / r^3$
$r^3 \sin \theta$	$2r \sin \theta$	$-2r \cos \theta$	$6r \sin \theta$
$r\theta \cos \theta$	$-2 \sin \theta / r$	0	0
$r \ln(r) \sin \theta$	$\sin \theta / r$	$-\cos \theta / r$	$\sin \theta / r$
$\sin \theta / r$	$-2 \sin \theta / r^3$	$2 \cos \theta / r^3$	$2 \sin \theta / r^3$
$r^{n+2} \cos n\theta$	$-(n+1)(n-2)r^n \cos n\theta$	$n(n+1)r^n \sin n\theta$	$(n+1)(n+2)r^n \cos n\theta$
$r^n \cos n\theta$	$-n(n-1)r^{n-2} \cos n\theta$	$n(n-1)r^{n-2} \sin n\theta$	$n(n-1)r^{n-2} \cos n\theta$
$r^{n+2} \sin n\theta$	$-(n+1)(n-2)r^n \sin n\theta$	$-n(n+1)r^n \cos n\theta$	$(n+1)(n+2)r^n \sin n\theta$
$r^n \sin n\theta$	$-n(n-1)r^{n-2} \sin n\theta$	$-n(n-1)r^{n-2} \cos n\theta$	$n(n-1)r^{n-2} \sin n\theta$

(Table 8.1 from Barber 2022)

We set rigid body motion components to zero for the displacements

Displacement Components

ϕ	$2\mu u_r$	$2\mu u_\theta$
r^2	$(\kappa - 1)r$	0
$r^2 \ln(r)$	$(\kappa - 1)r \ln(r) - r$	$(\kappa + 1)r\theta$
$\ln(r)$	$-1/r$	0
θ	0	$-1/r$
$r^3 \cos \theta$	$(\kappa - 2)r^2 \cos \theta$	$(\kappa + 2)r^2 \sin \theta$
$r\theta \sin \theta$	$\frac{1}{2}[(\kappa - 1)\theta \sin \theta - \cos \theta + (\kappa + 1) \ln(r) \cos \theta]$	$\frac{1}{2}[(\kappa - 1)\theta \cos \theta - \sin \theta - (\kappa + 1) \ln(r) \sin \theta]$
$r \ln(r) \cos \theta$	$\frac{1}{2}[(\kappa + 1)\theta \sin \theta - \cos \theta + (\kappa - 1) \ln(r) \cos \theta]$	$\frac{1}{2}[(\kappa + 1)\theta \cos \theta - \sin \theta - (\kappa - 1) \ln(r) \sin \theta]$
$\cos \theta / r$	$\cos \theta / r^2$	$\sin \theta / r^2$
$r^3 \sin \theta$	$(\kappa - 2)r^2 \sin \theta$	$-(\kappa + 2)r^2 \cos \theta$
$r\theta \cos \theta$	$\frac{1}{2}[(\kappa - 1)\theta \cos \theta + \sin \theta - (\kappa + 1) \ln(r) \sin \theta]$	$\frac{1}{2}[-(\kappa - 1)\theta \sin \theta - \cos \theta - (\kappa + 1) \ln(r) \cos \theta]$
$r \ln(r) \sin \theta$	$\frac{1}{2}[-(\kappa + 1)\theta \cos \theta - \sin \theta + (\kappa - 1) \ln(r) \sin \theta]$	$\frac{1}{2}[(\kappa + 1)\theta \sin \theta + \cos \theta + (\kappa - 1) \ln(r) \cos \theta]$
$\sin \theta / r$	$\sin \theta / r^2$	$-\cos \theta / r^2$
$r^{n+2} \cos n\theta$	$(\kappa - n - 1)r^{n+1} \cos n\theta$	$(\kappa + n + 1)r^{n+1} \sin n\theta$
$r^n \cos n\theta$	$-nr^{n-1} \cos n\theta$	$nr^{n-1} \sin n\theta$
$r^{n+2} \sin n\theta$	$(\kappa - n - 1)r^{n+1} \sin n\theta$	$-(\kappa + n + 1)r^{n+1} \cos n\theta$
$r^n \sin n\theta$	$-nr^{n-1} \sin n\theta$	$-nr^{n-1} \cos n\theta$

(Table 9.1 from Barber 2022)

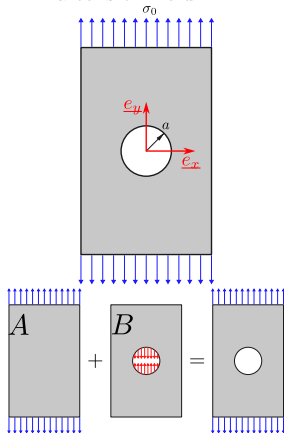
$$\text{Plane Stress } \kappa = \frac{3-\nu}{1+\nu}$$

$$\text{Plane Strain } \kappa = 3 - 4\nu$$

4.2.1. Plate With a Hole Under Tension

Linear Elastic Fracture Mechanics

- Let us now try to use the above table for obtaining the stress distribution around a hole in a tension field.

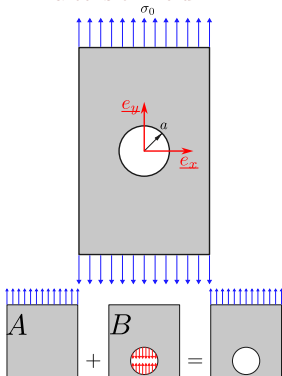


- We “decompose” the actual problem into two problems:
 - Problem A** Infinite plane under uniaxial tension.
 - Problem B** Infinite plane with compressive stresses on a circle of radius a .
- We will choose appropriate functions from the general solution for ϕ based on what we want the stress to look like.

4.2.1. Plate With a Hole Under Tension

Linear Elastic Fracture Mechanics

- Let us now try to use the above table for obtaining the stress distribution around a hole in a tension field.



Displacement Field

$$u_r = \frac{\sigma_0}{2}(\kappa - 1)r - \frac{\sigma_0}{2}r \cos 2\theta$$

$$u_\theta = \frac{\sigma_0}{2}r \sin 2\theta$$

Problem A

- In this case we already know the state of stress everywhere. This is

$$\underline{\underline{\sigma}}_{cart} = \begin{bmatrix} 0 & 0 \\ 0 & \sigma_0 \end{bmatrix}.$$

- Transforming to cylindrical coordinates,

$$\begin{aligned} \underline{\underline{\sigma}}_{cyl} &= \begin{bmatrix} \cos \theta & \sin \theta \\ -\sin \theta & \cos \theta \end{bmatrix} \begin{bmatrix} 0 & 0 \\ 0 & \sigma_0 \end{bmatrix} \begin{bmatrix} \cos \theta & -\sin \theta \\ \sin \theta & \cos \theta \end{bmatrix} \\ &= \sigma_0 \begin{bmatrix} \sin^2 \theta & \sin \theta \cos \theta \\ \sin \theta \cos \theta & \cos^2 \theta \end{bmatrix} \end{aligned}$$

The components can be written as

$$\sigma_{rr} = \sigma_0 \left(\frac{1}{2} - \frac{\cos 2\theta}{2} \right), \quad \sigma_{r\theta} = \sigma_0 \frac{\sin 2\theta}{2},$$

$$\sigma_{\theta\theta} = \sigma_0 \left(\frac{1}{2} + \frac{\cos 2\theta}{2} \right).$$

- Based on the table, we choose

$$\phi = \frac{\sigma_0}{4}r^2 + \frac{\sigma_0}{4}r^2 \cos 2\theta.$$

4.2.1. Plate With a Hole Under Tension

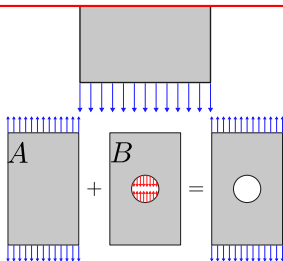
Linear Elastic Fracture Mechanics

- Let us now try to use the above table for obtaining the stress distribution around a hole in a tension field.

Displacement Field

$$u_r = \frac{\sigma_0 a^2}{2r} \left(1 - (\kappa + 1 - \frac{a^2}{r^2}) \cos 2\theta \right)$$

$$u_\theta = \frac{\sigma_0 a^2}{2r} \left(\kappa - 1 + (\frac{a}{r})^2 \right) \sin 2\theta.$$



Problem B

At $r = a$ we want

$$\sigma_{rr} = -\sigma_0 \left(\frac{1}{2} - \frac{\cos 2\theta}{2} \right), \quad \sigma_{r\theta} = -\sigma_0 \frac{\sin 2\theta}{2}.$$

(no hoop component specified)

As $r \rightarrow \infty$, we want $\sigma_{rr}, \sigma_{r\theta}, \sigma_{\theta\theta} \rightarrow 0$ to match the far-field.

- Based on inspection (shown in class), we find the following Airy stress function to be a good starting point: $\phi = A \log r + B\theta + C \cos 2\theta + D \frac{\cos 2\theta}{r^2}$.
- Solving for A, B, C, D based on the B.C.s we get,

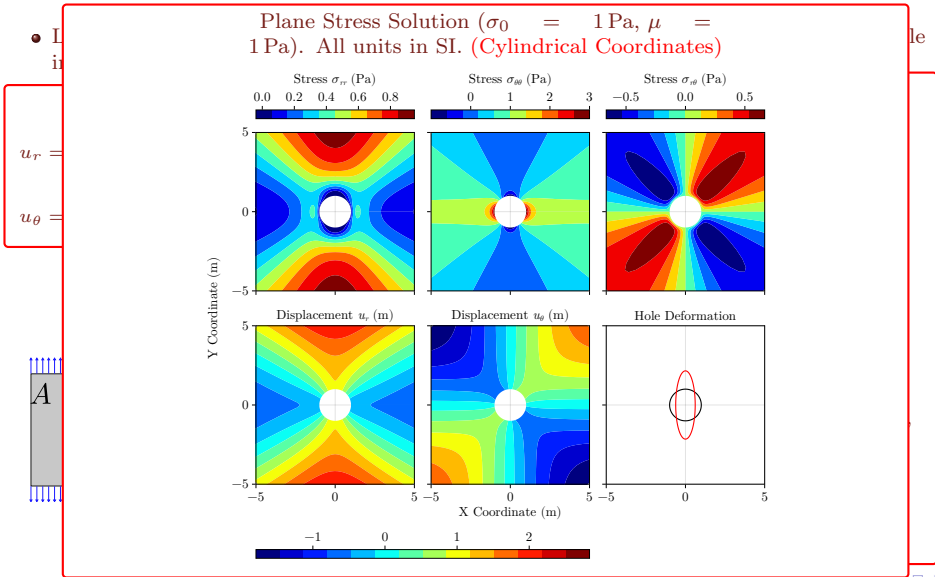
$$\sigma_{rr} = -\frac{\sigma_0}{2} \left(\frac{a}{r} \right)^2 + 2\sigma_0 \left(\frac{a}{r} \right)^2 \left(1 - \frac{3}{4} \left(\frac{a}{r} \right)^2 \right) \cos 2\theta,$$

$$\sigma_{\theta\theta} = \frac{\sigma_0}{2} \left(\frac{a}{r} \right)^2 + \frac{3\sigma_0}{2} \left(\frac{a}{r} \right)^4 \cos 2\theta,$$

$$\sigma_{r\theta} = \sigma_0 \left(\frac{a}{r} \right)^2 \left(1 - \frac{3}{2} \left(\frac{a}{r} \right)^2 \right) \sin 2\theta$$

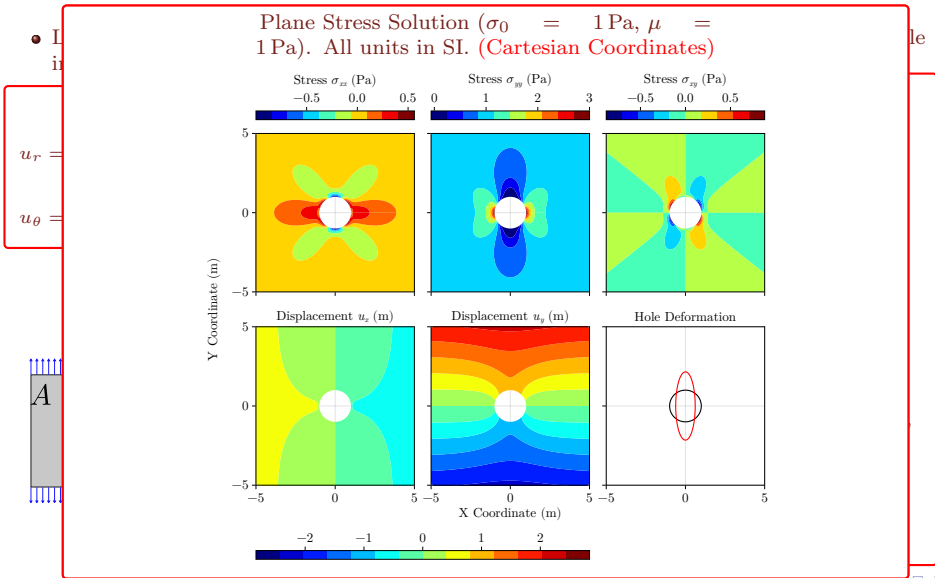
4.2.1. Plate With a Hole Under Tension

Linear Elastic Fracture Mechanics



4.2.1. Plate With a Hole Under Tension

Linear Elastic Fracture Mechanics



4.2.1. Plate with a Hole Under Uniaxial Tension

Classical Solutions

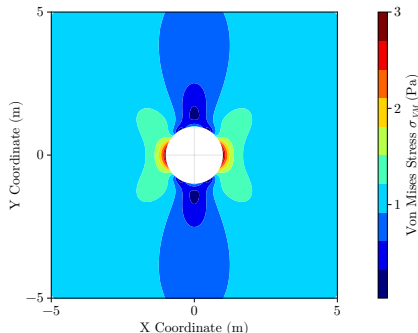
- Let us turn our attention towards the **Von Mises stress** now to understand how (and where) the plate will fail.
- It follows intuition that the maximum stresses will be attained close to the hole.
- The state of stress here ($r = a$) can be expressed as:

$$\sigma_{rr} = \sigma_{r\theta} = 0, \quad \sigma_{\theta\theta} = \sigma_0(1 + 2 \cos 2\theta)$$

(so $\sigma_{VM} = \sigma_{\theta\theta}$ here).

- The peak stress is achieved at $\theta = 0, \pi$, where $\sigma_{\theta\theta} = 3\sigma_0$.

Our MDE prediction for failure is that the plate will start tearing here.



The Distribution of the Von Mises Stress

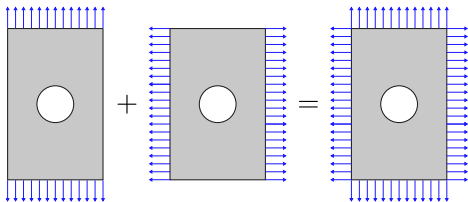
The Stress Concentration Factor (SCF)

Let us divide the **peak stress anywhere on the plate** ($3\sigma_0$ here) by the applied stress in the far-field (σ_0 here). This is known as the **Stress Concentration Factor (SCF)** and comes out to be 3 here.

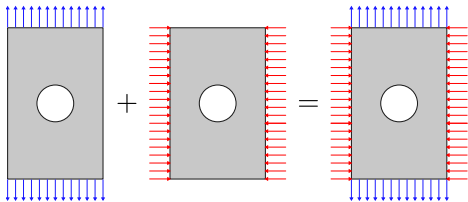
4.2.2. Plate with a Hole Under Biaxial Tension

Classical Solutions

Variant 1



Variant 2



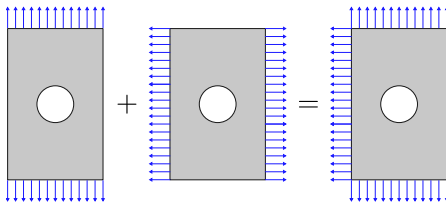
Variant 1 is fully tensile, Variant 2 is tensile in one direction and compressive in another.

- Now let us use the above solution to consider the same plate under a **biaxial state of stress**.
- The first adds a horizontal tensile component while the second adds a horizontal compressive component.
- We get the solution for tension in the horizontal direction by adding $\frac{\pi}{2}$ to the vertical direction tension solution from before.
- Adding the previous solution to this or subtracting this from the previous solution gives us the two variants.
- We can easily obtain the stress concentration factor since the maximum stresses occur at $r = a$ here also.

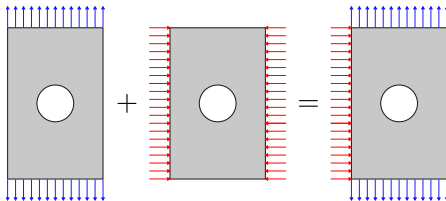
4.2.2. Plate with a Hole Under Biaxial Tension

Classical Solutions

Variant 1



Variant 2



Variant 1 is fully tensile, Variant 2 is tensile in one direction and compressive in another.

Variant 1

- The hoop stress is written as

$$\begin{aligned}\sigma_{\theta\theta} &= \sigma_0(1 + 2 \cos 2\theta) \\ &\quad + \sigma_0(1 + 2 \cos 2(\frac{\pi}{2} + \theta)) \\ &= 2\sigma_0,\end{aligned}$$

i.e., the hoop stress maintains a constant value of $2\sigma_0$.

- So the SCF for this is 2, **lesser** than the SCF of the uniaxial tension case!

Variant 2

- The hoop stress is written as

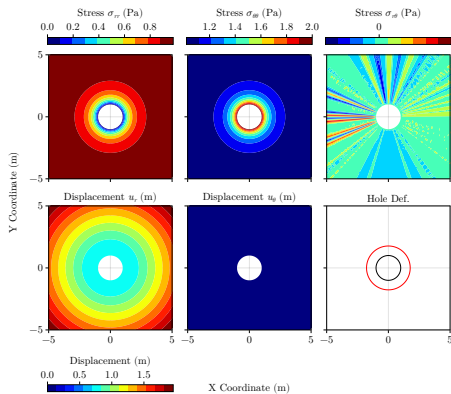
$$\begin{aligned}\sigma_{\theta\theta} &= \sigma_0(1 + 2 \cos 2\theta) \\ &\quad - \sigma_0(1 + 2 \cos 2(\frac{\pi}{2} + \theta)) \\ &= 4\sigma_0 \cos 2\theta.\end{aligned}$$

- The SCF is 4 here, **more** than the SCF of the uniaxial tension case!

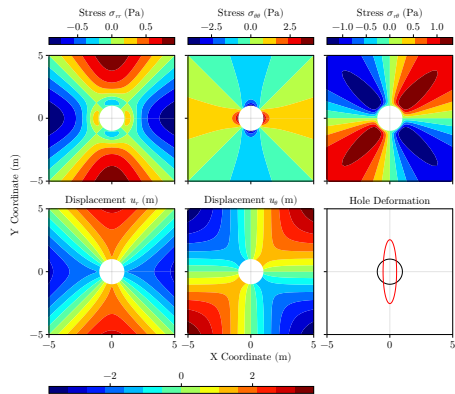
4.2.2. Plate with a Hole Under Biaxial Tension

Classical Solutions

Let us now visualize the solutions in each case.



Variant 1 (biaxial tension) - Cylindrical

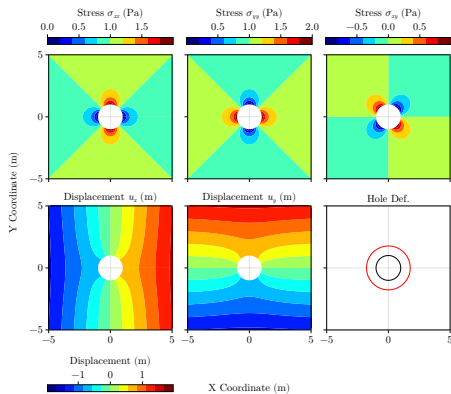


Variant 2 (tension in y; compression in x) - Cylindrical

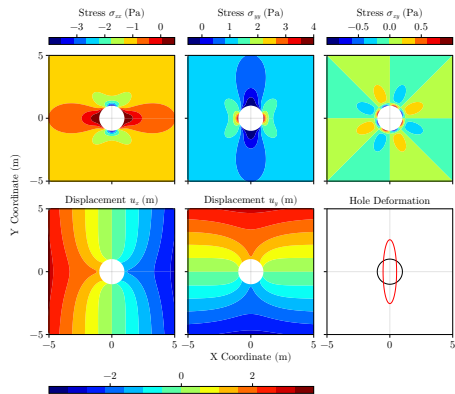
4.2.2. Plate with a Hole Under Biaxial Tension

Classical Solutions

Let us now visualize the solutions in each case.



Variant 1 (biaxial tension) - Cartesian

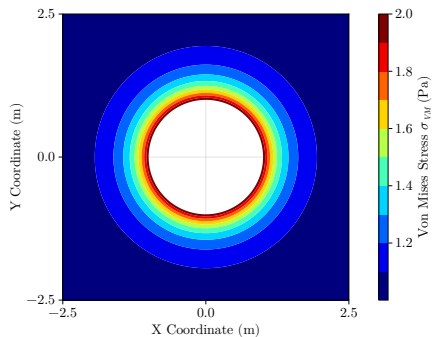


Variant 2 (tension in y; compression in x) - Cartesian

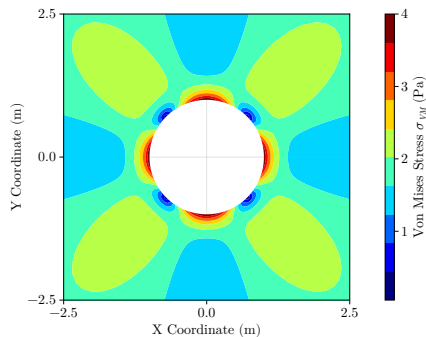
4.2.2. Plate with a Hole Under Biaxial Tension

Classical Solutions

Let us now visualize the solutions in each case.



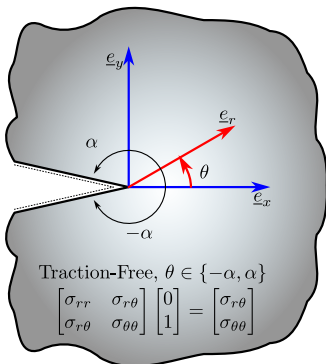
Variant 1 (biaxial tension) - Von Mises Stress



Variant 2 (tension in y; compression in x) - Von Mises Stress

4.2.3. Notch Crack

Classical Solutions



- Using the same approach, let us seek the stress distribution around a notch crack to understand when/how we may expect it to fail.
- Note that irrespective of what stress distribution we get, the strain energy has to be finite, and also the local deformation field has to be finite.
- Suppose $\sigma \sim \mathcal{O}(r^\lambda)$, $\varepsilon \sim \mathcal{O}(r^\lambda)$ necessarily.
 - So $\mathcal{U} = \int \int \frac{\sigma \varepsilon}{2} r dr d\theta \sim \mathcal{O}(r^{2\lambda+2})$.
 - For this to be finite for arbitrarily small r , it must be differentiable at 0. So $2\lambda + 1 \geq 0 \implies \lambda \geq -\frac{1}{2}$.
- We list out **the only Airy stress functions** that can show this in the following table (refer sl. 29).

ϕ	σ_{rr}	$\sigma_{r\theta}$	$\sigma_{\theta\theta}$
$r^{n+2} \cos n\theta$	$(..)r^n \cos n\theta$	$(..)r^n \sin n\theta$	$(..)r^n \cos n\theta$
$r^n \cos n\theta$	$(..)r^{n-2} \cos n\theta$	$(..)r^{n-2} \sin n\theta$	$(..)r^{n-2} \cos n\theta$
$r^{n+2} \sin n\theta$	$(..)r^n \sin n\theta$	$(..)r^n \cos n\theta$	$(..)r^n \sin n\theta$
$r^n \sin n\theta$	$(..)r^{n-2} \sin n\theta$	$(..)r^{n-2} \cos n\theta$	$(..)r^{n-2} \sin n\theta$

4.2.3. Singularity Close to Notch Crack

Classical Solutions

- For the Notch crack problem, we posit the following Airy stress function (so that stresses are all $\sim \mathcal{O}(r^\lambda)$).

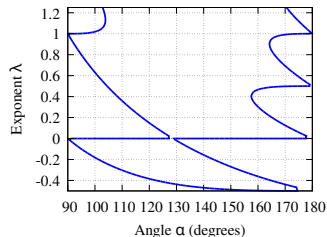
$$\phi = r^{\lambda+2} (A_1 \cos((\lambda + 2)\theta) + A_2 \cos(\lambda\theta) + B_1 \sin((\lambda + 2)\theta) + B_2 \sin(\lambda\theta)).$$

4.2.3. Singularity Close to Notch Crack

Classical Solutions

- For the Notch crack problem, we posit the following Airy stress function (so that stresses are all $\sim \mathcal{O}(r^\lambda)$).

$$\phi = r^{\lambda+2} (A_1 \cos((\lambda + 2)\theta) + A_2 \cos(\lambda\theta) + B_1 \sin((\lambda + 2)\theta) + B_2 \sin(\lambda\theta)) .$$



The general λ - α relationship (from the general boundary value problem). Going forward, Our interest is restricted to $\alpha \rightarrow \pi$ (so $\lambda = -0.5$).

4.2.3. Singularity Close to Notch Crack

Classical Solutions

- For the Notch crack problem, we posit the following Airy stress function (so that stresses are all $\sim \mathcal{O}(r^\lambda)$).

$$\phi = r^{\lambda+2} (A_1 \cos((\lambda + 2)\theta) + A_2 \cos(\lambda\theta) + B_1 \sin((\lambda + 2)\theta) + B_2 \sin(\lambda\theta)).$$

- Applying the boundary conditions (along with $\alpha = \pi$), we get a nonlinear eigenvalue problem that has the following solutions (recall that $\lambda \geq -\frac{1}{2}$ for energy finiteness):

λ_n	Eigenfunction
$-\frac{1}{2}$	$A_2 = 3A_1, B_2 = -B_1$
0	$A_2 = -A_1, B_1 = 0$ ($B_2 \neq 0$, but $\sin(\lambda\theta) = 0$)
$\frac{1}{2}$	$A_2 = -5A_1, B_2 = -B_1$
\vdots	\vdots
	$\cos(4\pi\lambda) = 1 \implies \lambda_n = \frac{n}{2}$

The exact solution is an infinite series that contains contributions from all the λ_n terms. Note, however, that as $r \rightarrow 0$, the $\lambda = -1/2$ terms will dominate.

This is a **singular stress field**, and its distribution ($\sigma \propto \frac{1}{\sqrt{r}}$) is *independent of the exact loading conditions!*

4.2.3. Singularity Close to Notch Crack

Classical Solutions

- For the Notch crack problem, we posit the following Airy stress function (so that stresses are all $\sim \mathcal{O}(r^\lambda)$).

$$\phi = r^{\lambda+2} (A_1 \cos((\lambda+2)\theta) + A_2 \cos(\lambda\theta) + B_1 \sin((\lambda+2)\theta) + B_2 \sin(\lambda\theta)).$$

- Applying the boundary conditions (along with $\alpha = \pi$), we get a nonlinear eigenvalue problem that has the following solutions (recall that $\lambda \geq -\frac{1}{2}$ for energy finiteness):

λ_n	Eigenfunction
$-\frac{1}{2}$	$A_2 = 3A_1, B_2 = -B_1$
0	$A_2 = -A_1, B_1 = 0$ ($B_2 \neq 0$, but $\sin(\lambda\theta) = 0$)
$\frac{1}{2}$	$A_2 = -5A_1, B_2 = -B_1$
\vdots	\vdots
	$\cos(4\pi\lambda) = 1 \implies \lambda_n = \frac{n}{2}$

- $\lambda = -\frac{1}{2}$ corresponds to the near-field singular stress field, given by

$$\sigma_{rr} = \frac{K_I}{\sqrt{2\pi r}} \left(\frac{5}{4} \cos \frac{\theta}{2} - \frac{1}{4} \cos \frac{3\theta}{2} \right) + \frac{K_{II}}{\sqrt{2\pi r}} \left(-\frac{5}{4} \sin \frac{\theta}{2} + \frac{3}{4} \sin \frac{3\theta}{2} \right)$$

$$\sigma_{\theta\theta} = \frac{K_I}{\sqrt{2\pi r}} \left(\frac{3}{4} \cos \frac{\theta}{2} + \frac{1}{4} \cos \frac{3\theta}{2} \right) + \frac{K_{II}}{\sqrt{2\pi r}} \left(-\frac{3}{4} \sin \frac{\theta}{2} - \frac{3}{4} \sin \frac{3\theta}{2} \right)$$

$$\sigma_{r\theta} = \frac{K_I}{\sqrt{2\pi r}} \left(\frac{1}{4} \sin \frac{\theta}{2} + \frac{1}{4} \sin \frac{3\theta}{2} \right) + \frac{K_{II}}{\sqrt{2\pi r}} \left(\frac{1}{4} \cos \frac{\theta}{2} + \frac{3}{4} \cos \frac{3\theta}{2} \right)$$

(We have replaced $A_1 = \frac{K_I}{3\sqrt{2\pi}}$ and $B_1 = -\frac{K_{II}}{\sqrt{2\pi}}$ to bring this to standard form)

4.2.3. Singularity Close to Notch Crack

Classical Solutions

- For the Notch crack problem, we posit the following Airy stress function (so that stresses are all $\sim \mathcal{O}(r^\lambda)$).

$$\phi = r^{\lambda+2} (A_1 \cos((\lambda+2)\theta) + A_2 \cos(\lambda\theta) + B_1 \sin((\lambda+2)\theta) + B_2 \sin(\lambda\theta)).$$

- Applying the boundary conditions (along with $\alpha = \pi$), we get a nonlinear eigenvalue problem that has the following solutions (recall that $\lambda \geq -\frac{1}{2}$ for energy finiteness):

λ_n | Eigenfunction

Displacement Field

$$2\mu u_r = K_I \sqrt{\frac{r}{2\pi}} \left((\kappa - \frac{1}{2}) \cos \frac{\theta}{2} - \frac{1}{2} \cos \frac{3\theta}{2} \right) - K_{II} \sqrt{\frac{r}{2\pi}} \left((\kappa - \frac{1}{2}) \sin \frac{\theta}{2} - \frac{3}{2} \sin \frac{3\theta}{2} \right)$$

$$2\mu u_\theta = K_I \sqrt{\frac{r}{2\pi}} \left(-(\kappa + \frac{1}{2}) \sin \frac{\theta}{2} + \frac{1}{2} \sin \frac{3\theta}{2} \right) - K_{II} \sqrt{\frac{r}{2\pi}} \left((\kappa + \frac{1}{2}) \cos \frac{\theta}{2} - \frac{3}{2} \cos \frac{3\theta}{2} \right)$$

- $\lambda = -\frac{1}{2}$ corresponds to the near-field singular stress field, given by

$$\sigma_{rr} = \frac{K_I}{\sqrt{2\pi r}} \left(\frac{5}{4} \cos \frac{\theta}{2} - \frac{1}{4} \cos \frac{3\theta}{2} \right) + \frac{K_{II}}{\sqrt{2\pi r}} \left(-\frac{5}{4} \sin \frac{\theta}{2} + \frac{3}{4} \sin \frac{3\theta}{2} \right)$$

$$\sigma_{\theta\theta} = \frac{K_I}{\sqrt{2\pi r}} \left(\frac{3}{4} \cos \frac{\theta}{2} + \frac{1}{4} \cos \frac{3\theta}{2} \right) + \frac{K_{II}}{\sqrt{2\pi r}} \left(-\frac{3}{4} \sin \frac{\theta}{2} - \frac{3}{4} \sin \frac{3\theta}{2} \right)$$

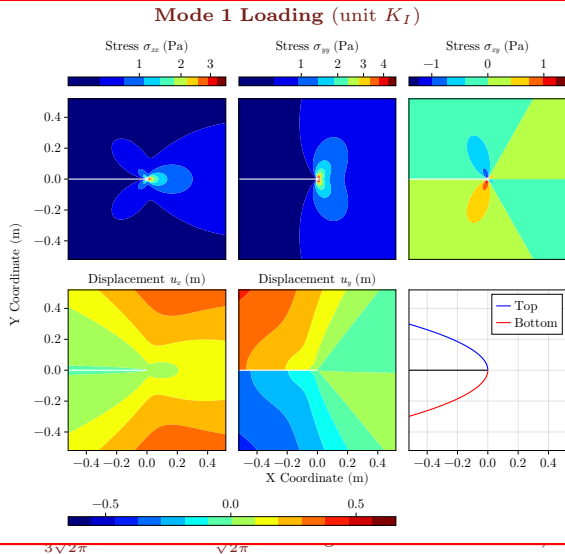
$$\sigma_{r\theta} = \frac{K_I}{\sqrt{2\pi r}} \left(\frac{1}{4} \sin \frac{\theta}{2} + \frac{1}{4} \sin \frac{3\theta}{2} \right) + \frac{K_{II}}{\sqrt{2\pi r}} \left(\frac{1}{4} \cos \frac{\theta}{2} + \frac{3}{4} \cos \frac{3\theta}{2} \right)$$

(We have replaced $A_1 = \frac{K_I}{3\sqrt{2\pi}}$ and $B_1 = -\frac{K_{II}}{\sqrt{2\pi}}$ to bring this to standard form)

4.2.3. Singularity Close to Notch Crack

Classical Solutions

- For the Notch crack problem we posit the following Airy stress function (so that stresses

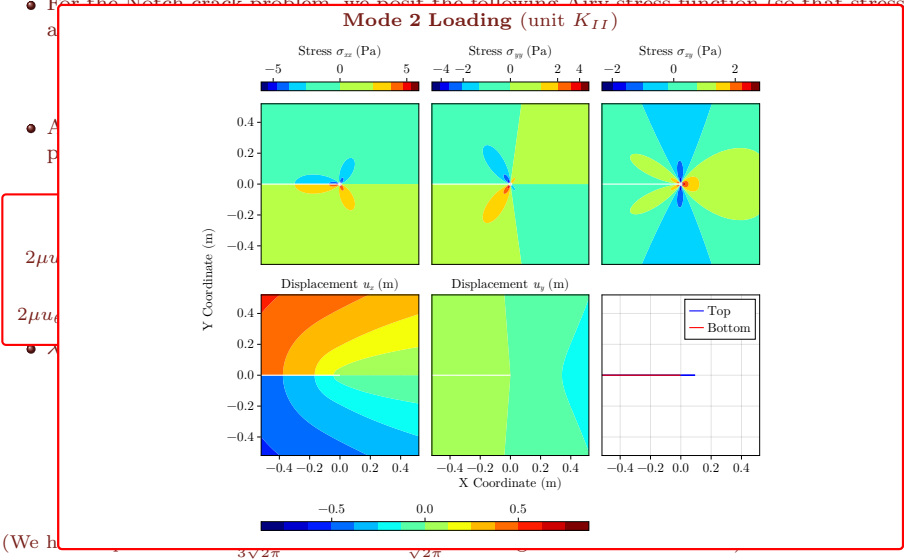


(We h

4.2.3. Singularity Close to Notch Crack

Classical Solutions

- For the Notch crack problem we posit the following Airy stress function (so that stresses



(We h

4.2. Classical Solutions

Linear Elastic Fracture Mechanics

- We now have a serious problem. The stress terms $\sigma \propto \frac{1}{\sqrt{r}}$ suggests a theoretical SCF of infinity irrespective of the loading!
- So by naive application of MNS/MDE, we would predict failure at notch location even for very small loads!
- Clearly there's a gap in the theory because this goes against practical experience.
- A. A. Griffith offered one of the earliest theories in terms of energy balance.
 - A crack will only grow if the locally stored energy crosses a threshold.
- The stress fields are parameterized in terms of the Stress Intensity Functions (SIFs) K_I and K_{II} .

4.2. Classical Solutions

Linear Elastic Fracture Mechanics

- We now have a serious problem. The stress terms $\sigma \propto \frac{1}{\sqrt{r}}$ suggests a theoretical SCF of infinity irrespective of the loading!
- So by naive application of MNS/MDE, we would predict failure at notch location even for very small loads!
- Clearly there's a gap in the theory because this goes against practical experience.
- A. A. Griffith offered one of the earliest theories in terms of energy balance.
 - A crack will only grow if the locally stored energy crosses a threshold.
- The stress fields are parameterized in terms of the Stress Intensity Functions (SIFs) K_I and K_{II} .

Crack Tip Stress Distribution in Cartesian Coordinates

$$\begin{aligned}\sigma_{xx} &= \frac{K_I}{\sqrt{2\pi r}} \left(\frac{3}{4} \cos \frac{\theta}{2} + \frac{1}{4} \cos \frac{5\theta}{2} \right) - \frac{K_{II}}{\sqrt{2\pi r}} \left(\frac{7}{4} \sin \frac{\theta}{2} + \frac{1}{4} \sin \frac{5\theta}{2} \right) \\ \sigma_{yy} &= \frac{K_I}{\sqrt{2\pi r}} \left(\frac{5}{4} \cos \frac{\theta}{2} - \frac{1}{4} \cos \frac{5\theta}{2} \right) - \frac{K_{II}}{\sqrt{2\pi r}} \left(\frac{1}{4} \sin \frac{\theta}{2} - \frac{1}{4} \sin \frac{5\theta}{2} \right) \\ \sigma_{xy} &= \frac{K_I}{\sqrt{2\pi r}} \left(-\frac{1}{4} \sin \frac{\theta}{2} + \frac{1}{4} \sin \frac{5\theta}{2} \right) + \frac{K_{II}}{\sqrt{2\pi r}} \left(\frac{3}{4} \cos \frac{\theta}{2} + \frac{1}{4} \cos \frac{5\theta}{2} \right).\end{aligned}$$

4.3. Griffith's Analysis and Energy Release Rate

Linear Elastic Fracture Mechanics

- In Module 1 we defined the **work potential** as

$$W = \Pi - U,$$

so that $\delta W = 0$ is the statement of the principle of virtual work for equilibrium.

- Here, Π corresponds to boundary work and U corresponds to body/internal work. In the strength of materials context, U is strain energy and Π is the contribution of boundary loads.
- In the early 1920s, A. A. Griffith argued that:
 - Propagation of a crack is the **creation of free surfaces that did not exist before**;
 - Since creating new surface area requires energy, this can be equated to the reduction in strain energy (or increase in work potential).
- If we parameterize the work potential in terms of the available exposed area (\mathcal{A}), we can mathematically express this energy balance as

$$W(\mathcal{A} + \Delta\mathcal{A}) - W(\mathcal{A}) = G\Delta\mathcal{A} \Rightarrow \boxed{\frac{\partial W}{\partial \mathcal{A}} = G},$$

where we define G as the *Griffith energy release rate*.

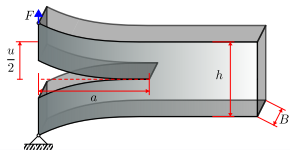
- $E_S(\mathcal{A}) = \mathcal{A}\gamma$ is a simplified expression of surface energy where γ is a material constant, so that $\Delta E_S = \gamma\Delta\mathcal{A}$.
- Griffith's principle, expressed mathematically, states that a crack can grow when the following equality is met:

$$\boxed{\frac{dW}{d\mathcal{A}} = \gamma}.$$

4.3. Griffith's Analysis and Energy Release Rate

Linear Elastic Fracture Mechanics

Let us work out the energy release rate for one of the simplest examples of crack propagation: the **Double Cantilever Beam (DCB)**.



Load-Displacement Relationship

$$\frac{u}{2} = F \frac{a^3}{3E'I} \implies \boxed{u = \frac{2a^3}{3E'I} F}$$

$$\text{with } E' = \begin{cases} E_y & \text{Plane Stress} \\ \frac{E_y}{1-\nu^2} & \text{Plane Strain} \end{cases}$$

If the crack advances by Δa , the new crack-front surface that gets created is $\Delta A = B\Delta a$, so $\frac{da}{dA} = \frac{1}{B}$.

Force Controlled Experiment

- Suppose the system is controlled by the force, the work potential is written as

$$\Pi = Fu \quad \text{and} \quad U = \frac{Fu}{2} \implies W = \frac{Fu}{2}$$

- Since u is the *derived quantity*, we express $u = \frac{2a^3}{3E'I} F$ and write

$$W = \frac{a^3}{3E'I} F^2 \implies \frac{dW}{dA} = \frac{a^2}{E'IB} F^2$$

Displacement Controlled Experiment

- Suppose the system is controlled by the displacement, the work potential is written as

$$\Pi = 0 \quad \text{and} \quad U = \frac{Fu}{2} \implies W = -\frac{Fu}{2}$$

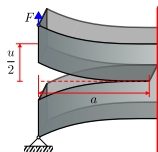
- Since F is the *derived quantity*, we write

$$W = -\frac{3E'I}{4a^3} u^2 \implies \frac{dW}{dA} = \frac{9E'I}{4a^4 B} u^2$$

4.3. Griffith's Analysis and Energy Release Rate

Linear Elastic Fracture Mechanics

Let us work out the energy release rate for one of the simplest examples of crack propagation: the **Double Cantilever Beam (DCB)**.



Load-Displacement

$$\frac{u}{2} = F \frac{a^3}{3E'I} \Rightarrow$$

$$\text{with } E' = \begin{cases} E_y & \text{Plane Stress} \\ \frac{E_y}{1-\nu^2} & \text{Plane Strain} \end{cases}$$

If the crack advances by Δa , the new crack-front surface that gets created is $\Delta A = B\Delta a$, so $\frac{dA}{da} = \frac{1}{B}$.

Force Controlled Experiment

- Suppose the system is controlled by the force, the work potential is written as

$$\Rightarrow W = \frac{Fu}{2}$$

ity, we express

$$U = \frac{a^2}{E'IB} F^2$$

Corollary: Let us analyze the stability of these cracks.

- Constant F : $\frac{dG}{da} = \frac{aF^2}{E'IB} > 0$, unstable.
- Constant u : $\frac{dG}{da} = -\frac{9E'I}{2a^5B} u^2 < 0$, stable.

Recall:

$$\frac{d^2W}{da^2} < 0 \text{ implies stability and}$$

$$\frac{d^2W}{da^2} > 0 \text{ implies instability.}$$

Experiment

- Suppose the system is controlled by the displacement, the work potential is written as

$$\Pi = 0 \quad \text{and} \quad U = \frac{Fu}{2} \Rightarrow W = -\frac{Fu}{2}$$

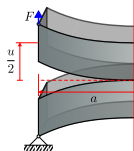
- Since F is the *derived quantity*, we write

$$W = -\frac{3E'I}{4a^3} u^2 \Rightarrow \frac{dW}{dA} = \frac{9E'I}{4a^4B} u^2$$

4.3. Griffith's Analysis and Energy Release Rate

Linear Elastic Fracture Mechanics

Let us work out the energy release rate for one of the simplest examples of crack propagation: the **Double Cantilever Beam (DCB)**.



Load-Displacement

$$\frac{u}{2} = F \frac{a^3}{3E'I}$$

$$\text{with } E' = \begin{cases} E_y & \text{Plane Stress} \\ \frac{E_y}{1-\nu^2} & \text{Plane Strain} \end{cases}$$

If the crack advances by Δa , the new crack-front surface that gets created is $\Delta A = B\Delta a$, so $\frac{dA}{da} = \frac{1}{B}$.

Force Controlled Experiment

- Suppose the system is controlled by the force, the work potential is written as

Finding the Stress Intensity Factor

Since the stresses close to the crack are dominated by the $\frac{1}{\sqrt{r}}$ singular stress fields (from the analytical treatment of the notched crack tip), we shall revert back to that solution and find the energy release rate there.

Equating that to the release rate obtained here will establish a relationship between the global loading condition (force F /displacement u here) and the SIF (K_I here).

displacement, the work potential is written as

$$\Pi = 0 \quad \text{and} \quad U = \frac{Fu}{2} \implies W = -\frac{Fu}{2}$$

- Since F is the *derived quantity*, we write

$$W = -\frac{3E'I}{4a^3}u^2 \implies \frac{dW}{dA} = \frac{9E'I}{4a^4B}u^2$$

$$\implies W = \frac{Fu}{2}$$

we express

$$= \frac{a^2}{E'IB}F^2$$

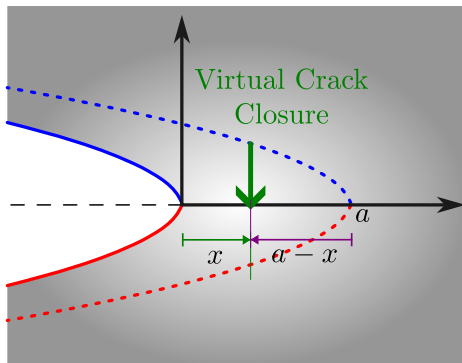
Experiment

controlled by the

4.3.3. Energy Release Rate

Griffith's Analysis and Energy Release Rate

- Since the notch crack geometry is infinite in all directions, **the energy released for a small crack growth will be equal to the energy required to close a crack by the same amount.**



4.3.3. Energy Release Rate

Griffith's Analysis and Energy Release Rate

- Since the notch crack geometry is infinite in all directions, **the energy released for a small crack growth will be equal to the energy required to close a crack by the same amount.**
- We observe that (all quantities in cylindrical):

$$\textcircled{\text{a}} \theta = 0, \quad \underline{\underline{\sigma}} = \frac{K_I}{\sqrt{2\pi r}} \begin{bmatrix} 1 & 0 \\ 0 & 1 \end{bmatrix} + \frac{K_{II}}{\sqrt{2\pi x}} \begin{bmatrix} 0 & 1 \\ 1 & 0 \end{bmatrix}, \quad 2\mu \underline{\underline{u}} = K_I \sqrt{\frac{r}{2\pi}} \begin{bmatrix} \kappa - 1 \\ 0 \end{bmatrix} - K_{II} \sqrt{\frac{r}{2\pi}} \begin{bmatrix} 0 \\ \kappa - 1 \end{bmatrix}$$

$$\textcircled{\text{a}} \theta = \pi, \quad \underline{\underline{\sigma}} = \frac{K_{II}}{\sqrt{2\pi r}} \begin{bmatrix} -2 & 0 \\ 0 & 0 \end{bmatrix}, \quad 2\mu \underline{\underline{u}} = K_I \sqrt{\frac{r}{2\pi}} \begin{bmatrix} 0 \\ -(\kappa + 1) \end{bmatrix} - K_{II} \sqrt{\frac{r}{2\pi}} \begin{bmatrix} \kappa + 1 \\ 0 \end{bmatrix}.$$

4.3.3. Energy Release Rate

Griffith's Analysis and Energy Release Rate

- Since the notch crack geometry is infinite in all directions, **the energy released for a small crack growth will be equal to the energy required to close a crack by the same amount.**
- We observe that (all quantities in cylindrical):

$$\text{@ } \theta = 0, \quad \underline{\underline{\sigma}} = \frac{K_I}{\sqrt{2\pi r}} \begin{bmatrix} 1 & 0 \\ 0 & 1 \end{bmatrix} + \frac{K_{II}}{\sqrt{2\pi x}} \begin{bmatrix} 0 & 1 \\ 1 & 0 \end{bmatrix}, \quad 2\mu \underline{u} = K_I \sqrt{\frac{r}{2\pi}} \begin{bmatrix} \kappa - 1 \\ 0 \end{bmatrix} - K_{II} \sqrt{\frac{r}{2\pi}} \begin{bmatrix} 0 \\ \kappa - 1 \end{bmatrix}$$

$$\text{@ } \theta = \pi, \quad \underline{\underline{\sigma}} = \frac{K_{II}}{\sqrt{2\pi r}} \begin{bmatrix} -2 & 0 \\ 0 & 0 \end{bmatrix}, \quad 2\mu \underline{u} = K_I \sqrt{\frac{r}{2\pi}} \begin{bmatrix} 0 \\ -(\kappa + 1) \end{bmatrix} - K_{II} \sqrt{\frac{r}{2\pi}} \begin{bmatrix} \kappa + 1 \\ 0 \end{bmatrix}.$$

- For virtual crack closure of just one half (say, the top), the work done can be written as (traction at $\theta = 0$ times negative displacement at $\theta = \pi$),

$$\begin{aligned} W(a) &= \int_0^a \left([\sigma_{r\theta} \quad \sigma_{\theta\theta}] \Big|_{\theta=0} \begin{bmatrix} -u_\theta \\ -u_r \end{bmatrix} \Big|_{\theta=\pi} \right) B dx \\ &= B \int_0^a \frac{K_I}{\sqrt{2\pi x}} K_I \sqrt{\frac{a-x}{2\pi}} \frac{\kappa+1}{2\mu} + \frac{K_{II}}{\sqrt{2\pi r}} K_{II} \sqrt{\frac{a-x}{2\pi}} \frac{\kappa+1}{2\mu} dx \\ &= B \frac{K_I^2 + K_{II}^2}{2\pi} \frac{\kappa+1}{2\mu} \int_0^a \sqrt{\frac{a-x}{x}} dx = \frac{K_I^2 + K_{II}^2}{8\mu} (\kappa+1) Ba = \frac{K_I^2 + K_{II}^2}{E'} Ba, \end{aligned}$$

where B is the out-of-plane dimension (thickness).

4.3.3. Energy Release Rate

Griffith's Analysis and Energy Release Rate

- Since the notch crack geometry is infinite in all directions, **the energy released for a small crack growth will be equal to the energy required to close a crack by the same amount.**

- We observe that (all quantities in cylindrical):

The Griffith Energy Release Rate is the derivative $\frac{dW}{dA} = \frac{dW}{da} \frac{da}{dA} = \lim_{a \rightarrow 0} \frac{1}{B} \frac{dW}{da}$, which evaluates as

$$G = \frac{K_I^2 + K_{II}^2}{E'}$$

with $E' = \begin{cases} E_y & \text{Plane stress} \\ \frac{E_y}{1-\nu^2} & \text{Plane strain} \end{cases}$

where $\kappa = \begin{cases} 0 & \text{Plane stress} \\ 1 & \text{Plane strain} \end{cases}$

- For virtual (traction at the crack tip) the energy release rate can be written as
- Note that the area \mathcal{A} is just the “crack front area” by convention, NOT the total area.

$$\begin{aligned}
 W(a) &= \int_0^a \left([\sigma_{r\theta} \quad \sigma_{\theta\theta}] \Big|_{\theta=0} \begin{bmatrix} -u_\theta \\ -u_r \end{bmatrix} \Big|_{\theta=\pi} \right) B dx \\
 &= B \int_0^a \frac{K_I}{\sqrt{2\pi x}} K_I \sqrt{\frac{a-x}{2\pi}} \frac{\kappa+1}{2\mu} + \frac{K_{II}}{\sqrt{2\pi r}} K_{II} \sqrt{\frac{a-x}{2\pi}} \frac{\kappa+1}{2\mu} dx \\
 &= B \frac{K_I^2 + K_{II}^2}{2\pi} \frac{\kappa+1}{2\mu} \int_0^a \sqrt{\frac{a-x}{x}} dx = \frac{K_I^2 + K_{II}^2}{8\mu} (\kappa+1) Ba = \frac{K_I^2 + K_{II}^2}{E'} Ba,
 \end{aligned}$$

where B is the out-of-plane dimension (thickness).

4.3.1. Stress Intensity Factor

Griffith's Analysis and Energy Release Rate

- A crack is said to propagate when G exceeds G_{cr} .
- Therefore, under “pure” mode 1 loading, the *Critical Stress Intensity Factor* ($K_{I,cr}$) is

$$K_{I,cr} = \sqrt{G_{cr} E'}.$$

- The general relationship of K_I, K_{II} to the far-field “applied” stresses is very closely tied in to the exact geometry, loading conditions, etc.
- For the DCB, which undergoes mode 1 loading, we have

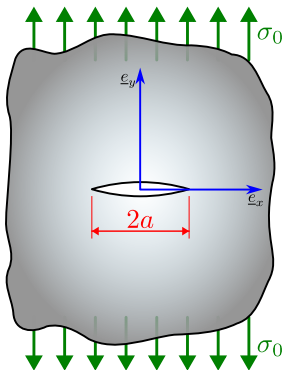
$$\frac{K_I^2}{E'} = \frac{a^2 F^2}{E' I B} \implies \boxed{K_I = \frac{a F}{\sqrt{I B}}}, \text{ and } \frac{K_I^2}{E'} = \frac{9 E' I}{4 a^4 B} u^2 \implies \boxed{K_I = \frac{3 E'}{2 a^2} \sqrt{\frac{I}{B}} u}$$

showing that the strength of the singularity is directly proportional to the applied load F or the imposed displacement u as the case may be.

- From the above expression for $K_{I,cr}$, one can easily back-calculate F_{cr} or u_{cr} , i.e., the critical load or the critical displacement for crack growth.
- Exact expressions for $K_I(F)$ exist for some classical examples, but in a lot of cases (especially after the advent of modern computing) numerical approaches have grown in popularity.

4.3.1. Griffith-Inglis Crack Revisited

Griffith's Analysis and Energy Release Rate



- For the flat crack of length $2a$ (aka the Griffith-Inglis crack), the SIF is related to tensile stresses by

$$K_I = \sigma_0 \sqrt{\pi a}.$$

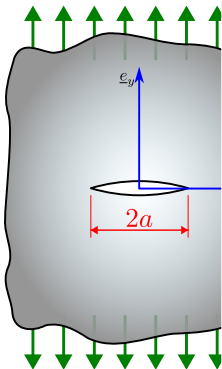
(The derivation involves the “Westergaard” complex potential approach, see Gdoutos 2005)

- Note that this is why we chose $\lambda = \frac{\pi}{2}$ in sl. 7. If we left it in, we'll have to satisfy (plane stress considered here):

$$\frac{4\lambda a}{E} \sigma_0^2 = \frac{2K_I^2}{E} = \frac{2\pi a}{E} \sigma_0^2.$$

4.3.1. Griffith-Inglis Crack Revisited

Griffith's Analysis and Energy Release Rate



Additional Cases to Consider

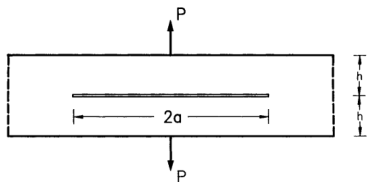


(Figure 4.23 from Gdoutos (2005))

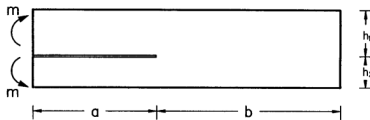


(Figure 4.20 from Gdoutos (2005))

the Griffith-Inglis crack),
by

“gaard” complex
(5)

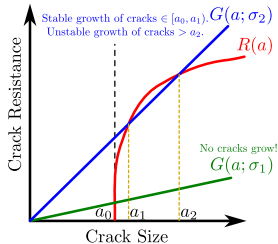
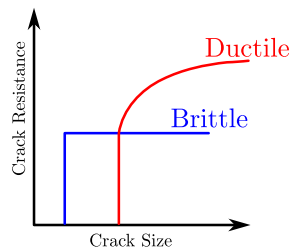
in sl. 7. If we left it in,
considered here):

$$\frac{\pi a}{E} \sigma_0^2.$$

4.4. Crack Propagation in Practice

Conditions for Unstable Crack Growth

- The critical energy release rate is empirically also found to be a function of the size of the crack.
- Since this is an important material constant, this is christened the **Crack Resistance**, denoted R .
- In some cases, cracks below a critical size do not grow, and crack propagation kicks in only after such a critical size.
- For **brittle materials**, the classical Griffith analysis is very closely valid (G_{cr} or R being independent of crack size).
- For **ductile materials**, strong size dependence is observed - this is due to the presence of a significant plastic zone in the vicinity of the crack tip (stresses are never really singular).



- The “R-curve” can be used to assess the stability of a crack under any given loading condition.
- $G \propto \sigma_0^2 a$ usually. So it is possible to use this plot to determine stable vs unstable crack growth.
- **Stable crack growth** when $G > R$ (crack size increases and stops)
- **Unstable crack growth** when $G > R$ and $\frac{dG}{da} > \frac{dR}{da}$ (crack size increases indefinitely).

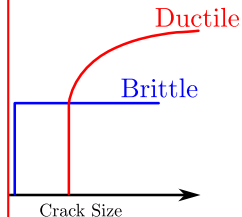
4.4. Crack Propagation in Practice

Conditions for Unstable Crack Growth

- The critical energy release rate is empirically also found to be a function of the crack size
- Since this is an implicit function, we have christened the G_{cr} as the **Crack Resistance**
- In some cases, crack growth is stable and crack propagation stops
- For **brittle materials**, the G_{cr} is closely valid ($G_{cr} \approx R$)
- For **ductile materials**, this is due to the plasticity in the vicinity of the crack tip

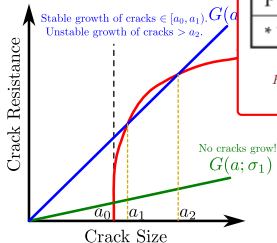
Material	G_{Ic} (J/m ²)
Mild Steel	≈250,000
Alloy Steel ($\sigma_{ys}^* = 1070$)	30,000
EN 24 (U.K.)	
4340 (U.S.A.)	
40Ni2Cr1Mo28 (I.S.)	
Aluminum 7075-T6	8,000
Titanium Ti-6Al-4V	29,000
Perspex (PMMA)	800
PVC	4,500

Representative G_{cr} values (table 2.3 from Kumar 2009).



the stability of a crack

use this plot to
growth.



- **Stable crack growth** when $G > R$ (crack size increases and stops)
- **Unstable crack growth** when $G > R$ and $\frac{dG}{da} > \frac{dR}{da}$ (crack size increases indefinitely).

4.4. Crack Propagation in Practice: Fatigue-Driven Growth

Linear Elastic Fracture Mechanics

- Supposing the applied load corresponds to stresses varying between σ_{\max} and σ_{\min} . We can transform this (based on the geometry, etc.) to SIFs K_{\max} and K_{\min} .
- Given K_{\max} , K_{\min} , the engineer is concerned with the question: **how much crack growth will be seen after a single cycle of load application?**
- **Paris Law:** $\frac{da}{dN} = C(\Delta K)^m$.
Here $\Delta K = K_{\max} - K_{\min}$ (expressed in $\text{MPa}\sqrt{\text{m}}$), and a is the crack length (expressed in m).
- Usually a_f is specified and we are interested in finding how many cycles until a crack of size a_i grows to a_f . This is the “life” of the structure.

Values for common engineering materials, from Kumar 2009

Material	C	m
Ferrite-Pearlite (S)	6.8×10^{-12}	3.0
Martensite (S)	1.33×10^{-10}	2.25
Austenite (S)	5.5×10^{-12}	3.25
Cast Iron (S)	4.3×10^{-8}	4
Al-Alloy	1.1×10^{-11}	3.89

4.5. The Plastic Zone - A Primer on Elastic Plastic Fracture Mechanics

Linear Elastic Fracture Mechanics

- The stress expressions developed for the notch crack predict a **stress singularity**, but when stresses exceed a threshold, the material behaves plastically.
- A simplistic analysis of this can be achieved by the elastic-perfectly plastic model.
- We can estimate a “plastic zone” around the crack by finding the contour $r(\theta)$ where the Von Mises stress is equal to the material yield stress S_y .

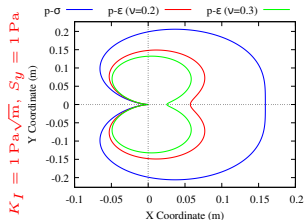
Mode 1 Crack ($K_{II} = 0$)

- Plane Stress

$$\sigma_{VM} = \frac{K_I}{2\sqrt{2\pi r}} \sqrt{(1 + \cos \theta)(5 - 3 \cos \theta)}$$

- Plane Strain

$$\sigma_{VM} = \frac{K_I}{2\sqrt{2\pi r}} \sqrt{(1 + \cos \theta)(5 - 3 \cos \theta + 8\nu(1 + \nu))}$$



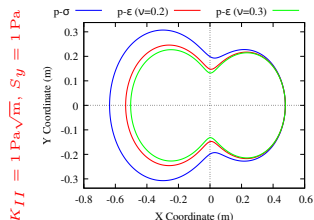
Mode 2 Crack ($K_I = 0$)

- Plane Stress

$$\sigma_{VM} = \frac{K_{II}}{4\sqrt{\pi r}} \sqrt{19 - 4 \cos \theta + 9 \cos 2\theta}$$

- Plane Strain

$$\sigma_{VM} = \frac{K_{II}}{4\sqrt{\pi r}} \sqrt{19 - 4 \cos \theta + 9 \cos 2\theta + 16\nu(1 + \nu)}$$



4.5. The Plastic Zone - A Primer on Elastic Plastic Fracture Mechanics

Linear Elastic Fracture Mechanics

- The stress expressions developed for the notch crack predict a **stress singularity**, but when strain hardening is included, the stress singularity is removed.
- A simplified model of the plastic zone is often used to estimate the fracture toughness of a material.
- We can estimate the size of the plastic zone by using the Von Mises stress criterion. The plastic zone is defined as the region where the stress is greater than the yield stress S_y .

These are $r(\theta)$ contours corresponding to $\sigma_{VM} = S_y$. A larger plastic zone implies more fracture toughness and a smaller plastic zone implies lesser fracture toughness.

An interesting consequence of this is that the fracture toughness of thin plates is higher than that of very thick plates!

Mode I Crack

- Plane Stress

$$\sigma_{VM} = \frac{K_I}{2\sqrt{2\pi r}} \sqrt{(1 + \cos\theta)(5 - 3\cos\theta)}$$

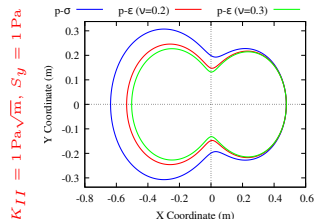
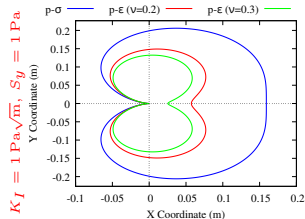
$$\sigma_{VM} = \frac{K_{II}}{4\sqrt{\pi r}} \sqrt{19 - 4\cos\theta + 9\cos 2\theta}$$

- Plane Strain

$$\sigma_{VM} = \frac{K_I}{2\sqrt{2\pi r}} \sqrt{(1 + \cos\theta)(5 - 3\cos\theta + 8\nu(1 + \nu))}$$

- Plane Strain

$$\sigma_{VM} = \frac{K_{II}}{4\sqrt{\pi r}} \sqrt{19 - 4\cos\theta + 9\cos 2\theta + 16\nu(1 + \nu)}$$



4.5. The Plastic Zone - A Primer on Elastic Plastic Fracture Mechanics

Linear Elastic Fracture Mechanics

- The stress expressions developed for the notch crack predict a **stress singularity**, but when str

These are $r(\theta)$ contours corresponding to $\sigma_{VM} = S_y$

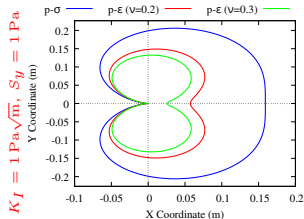
Plastic Zone Radii: First Order Estimates

- By setting $\sigma_{VM} = S_y$, we can obtain a measure of the plastic zone size by setting $\theta = 0$ for mode 1 and $\theta = \frac{\pi}{2}$ for mode 2.
- This turns out as:

$$r_y^{(I)} = \frac{K_I^2}{2\pi S_y^2} \begin{cases} 1 \\ (1 - 2\nu)^2 \end{cases}, \quad r_y^{(II)} = \frac{K_{II}^2}{8\pi S_y^2} \begin{cases} 5 \\ 5 - 8\nu(1 - \nu) \end{cases} \begin{array}{l} \text{Plane } \sigma \\ \text{Plane } \varepsilon \end{array} \cos^2 \theta$$

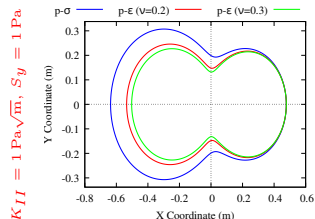
- Plane Strain

$$\sigma_{VM} = \frac{K_I}{2\sqrt{2\pi r}} \sqrt{(1 + \cos \theta)(5 - 3 \cos \theta + 8\nu(1 + \nu))}$$



- Plane Strain

$$\sigma_{VM} = \frac{K_{II}}{4\sqrt{\pi r}} \sqrt{19 - 4 \cos \theta + 9 \cos^2 \theta + 16\nu(1 + \nu)}$$



4.5. The Plastic Zone - A Primer on Elastic Plastic Fracture Mechanics

Linear Elastic Fracture Mechanics

- The stress expressions developed for the notch crack predict a **stress singularity**, but when str

These are $r(\theta)$ contours corresponding to $\sigma_{VM} = S_y$ A

Plastic Zone Radii: First Order Estimates

- By setting $\sigma_{VM} = S_y$, we can obtain a measure of the plastic zone size by setting $\theta = 0$ for mode 1 and $\theta = \frac{\pi}{2}$ for mode 2.
- This turns out as:

$$r_y^{(I)} = \frac{K_I^2}{2\pi S_y^2} \begin{cases} 1 & \text{Plane } \sigma \\ (1 - 2\nu)^2 & \text{Plane } \epsilon \end{cases}, \quad r_y^{(II)} = \frac{K_{II}^2}{8\pi S_y^2} \begin{cases} 5 & \text{Plane } \sigma \\ 5 - 8\nu(1 - \nu) & \text{Plane } \epsilon \end{cases}$$

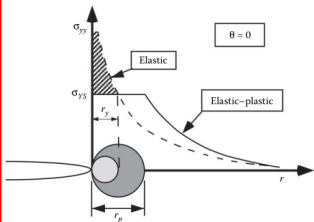


Figure 2.29 from Anderson 2017

- The **Irwin correction** tries to account for the stress redistribution for equilibrium due to the plastic zone.
- This gives larger estimates for the plastic radii:

$$r_p^{(I)} = \frac{K_I^2}{\pi S_y^2} \begin{cases} 1 & \text{Plane Stress} \\ 1 - 2\nu & \text{Plane Strain} \end{cases}$$

$$r_p^{(II)} = \frac{K_{II}^2}{2\pi S_y^2} \begin{cases} \sqrt{5} & \text{Plane Stress} \\ \sqrt{5 - 8\nu(1 - \nu)} & \text{Plane Strain} \end{cases}$$

4.6. Things We Have Not Considered

Linear Elastic Fracture Mechanics

- **The Effective Crack Concept** : A simpler way of tackling Elastic-Plastic Fracture Mechanics (EPFM) is by abstracting the plastic stress distribution away by considering an “effectively larger crack” around which the LEFM stress predictions will be identical to the EPFM stress predictions in some sense.
- **The J-Integral** : Line integral of the work potential over some path beginning at one face of a crack and ending on another. This formalizes the energy required for crack growth. For LEFM this is identical to *Griffith's energy release rate*. Things change when considering plasticity.
- **Crack Tip Opening Displacement (COD)** : The displacement close to the crack tip gets “frozen” due to plasticity near the crack tip. We can use the Irwin plastic zone estimate to obtain expressions for this permanent deformation. This will also grow with the SIF and can be used as a criterion for fracture.

5.1. Stress for Fatigue Life Estimation

Tutorial Problems

A 40 mm diameter solid circular bar is made from an aluminum alloy with the following fatigue properties (for the Basquin relationship): $\sigma'_f = 500$ MPa (fatigue strength coefficient), $b = -0.10$ (fatigue strength exponent), $S_{ult} = 320$ MPa (ultimate tensile strength).

- The bar is subjected to fully reversed (zero mean stress) cyclic axial loading. For an applied alternating force amplitude of $F_a = 100$ kN, estimate the number of cycles to fatigue failure using the Basquin relationship. (48×10^6)
- Now consider the case where an additional mean tensile force of $\sigma_m = 10$ kN is imposed along with the alternating load. Use the Goodman relationship with $m = 1.0$ and estimate the life. (37×10^6)

5.1. Stress for Fatigue Life Estimation

Tutorial Problems

Consider a cast iron DCB specimen with half-height (height of each beam) 20 mm, width 20 mm with an initial crack size of 80 mm, undergoing mode-I loading (force controlled). Assume plane stress is applicable (with $E_y = 200$ GPa), and take Paris law coefficients as $C = 4.3 \times 10^{-8}$, $m = 4$.

- Find the maximum alternating force the structure can support if the crack should not grow beyond 5% over 10^6 cycles. (110.04 N)
- Suppose that the critical G value is 250×10^3 Pam. Estimate the safe static load. (45.64 kN)

References I

- [1] Emmanuël Gdoutos. **Fracture Mechanics: An Introduction**, Second Edition. Solid Mechanics and Its Applications 123. Dordrecht: Springer Netherlands, 2005. ISBN: 978-1-4020-2863-2 978-1-4020-3153-3. DOI: [10.1007/1-4020-3153-X](https://doi.org/10.1007/1-4020-3153-X) (cit. on pp. **2**, **92**, **93**).
- [2] S. Suresh. **Fatigue of Materials**, 2nd ed. Cambridge ; New York: Cambridge University Press, 1998. ISBN: 978-0-521-57046-6 978-0-521-57847-9 (cit. on p. **2**).
- [3] William D. Callister Jr and David G. Rethwisch. **Fundamentals of Materials Science and Engineering: An Integrated Approach**, John Wiley & Sons, 2012. ISBN: 978-1-118-06160-2 (cit. on pp. **2**, **11–17**).
- [4] Prashant Kumar. **Elements of Fracture Mechanics**, 1st Edition. McGraw-Hill Education, 2009. ISBN: 978-0-07-065696-3. (Visited on 12/15/2024) (cit. on pp. **2**, **18–21**, **26**, **94–96**).
- [5] T. H. G. Megson. **Aircraft Structures for Engineering Students**, Elsevier, 2013. ISBN: 978-0-08-096905-3 (cit. on pp. **2**, **11–17**, **42–44**, **46**, **47**, **49**, **50**).
- [6] Sparky. *Sparky's Sword Science: Introduction to Crystal Structure*. Dec. 2013. (Visited on 08/09/2024) (cit. on pp. **3–5**).
- [7] *New Technique Provides Detailed Views of Metals' Crystal Structure*. <https://news.mit.edu/2016/metals-crystal-structure-0706>. July 2016. (Visited on 08/09/2024) (cit. on pp. **3–5**).
- [8] V Rajendran. **Materials Science**, Tata McGraw-Hill Education, 2011. ISBN: 978-1-259-05006-0 (cit. on pp. **6–10**).
- [9] Nick Connor. *What Is Stress-strain Curve - Stress-strain Diagram - Definition*. <https://material-properties.org/what-is-stress-strain-curve-stress-strain-diagram-definition/>. July 2020. (Visited on 08/07/2024) (cit. on pp. **6**, **7**).
- [10] *What Is Metal Fatigue? Metal Fatigue Failure Examples*. Apr. 2021. (Visited on 08/09/2024) (cit. on pp. **11–17**).
- [11] *The deHavilland Comet Disaster*. July 2019. (Visited on 08/09/2024) (cit. on pp. **11–17**).
- [12] *DCA21FA085.Aspx*. <https://www.nts.gov/investigations/Pages/DCA21FA085.aspx>. Aug. 2024. (Visited on 08/09/2024) (cit. on pp. **11–17**).
- [13] *Fatigue Physics*. Aug. 2024. (Visited on 08/09/2024) (cit. on pp. **11–17**).
- [14] Martin H. Sadd. **Elasticity: Theory, Applications, and Numerics**, 2nd ed. Amsterdam ; Boston: Elsevier/AP, 2009. ISBN: 978-0-12-374446-3 (cit. on pp. **22–25**).

References II

- [15] Richard G. Budynas, J. Keith Nisbett, and Joseph Edward Shigley. **Shigley's Mechanical Engineering Design**, Tenth edition. McGraw-Hill Series in Mechanical Engineering. New York, NY: McGraw-Hill Education, 2015. ISBN: 978-0-07-339820-4 (cit. on pp. **27**, **42–45**, **48–50**).
- [16] Yukitaka Murakami et al. “Essential Structure of *S-N* Curve: Prediction of Fatigue Life and Fatigue Limit of Defective Materials and Nature of Scatter”. **International Journal of Fatigue**, **146**, (May 2021), pp. 106138. ISSN: 0142-1123. DOI: [10.1016/j.ijfatigue.2020.106138](https://doi.org/10.1016/j.ijfatigue.2020.106138). (Visited on 04/13/2026) (cit. on p. **48**).
- [17] “De Havilland Comet”. **Wikipedia**, (Apr. 2025). (Visited on 04/08/2025) (cit. on pp. **52–54**).
- [18] J. R. Barber. **Elasticity**, vol. 172. Solid Mechanics and Its Applications. Cham: Springer International Publishing, 2022. ISBN: 978-3-031-15213-9 978-3-031-15214-6. DOI: [10.1007/978-3-031-15214-6](https://doi.org/10.1007/978-3-031-15214-6). (Visited on 12/17/2024) (cit. on pp. **59–61**).
- [19] Ted L. Anderson. **Fracture Mechanics: Fundamentals and Applications, Fourth Edition**, 4th ed. Boca Raton: CRC Press, Mar. 2017. ISBN: 978-1-315-37029-3. DOI: [10.1201/9781315370293](https://doi.org/10.1201/9781315370293) (cit. on pp. **97–100**).